Crosstalk between chloroplast thioredoxin systems in regulation of photosynthesis

Short title: Thioredoxin networks in chloroplasts

Lauri Nikkanen, Jouni Toivola and Eevi Rintamäki[1]

Molecular Plant Biology, Department of Biochemistry, University of Turku, FI-20014 Turku, Finland

[1]Corresponding author:
Eevi Rintamäki
evirin@utu.fi
Molecular Plant Biology
Department of Biochemistry
University of Turku
FI-20014 TURKU
Finland
+35823335568

Word count: 7568

ABSTRACT

Thioredoxins (TRXs) mediate light-dependent activation of primary photosynthetic reactions in plant chloroplasts by reducing disulphide bridges in redox-regulated enzymes. Of the two plastid TRX systems, the ferredoxin-TRX system consists of ferredoxin-thioredoxin reductase (FTR) and multiple TRXs, while the NADPH-dependent thioredoxin reductase (NTRC) contains a complete TRX system in a single polypeptide. Using Arabidopsis plants overexpressing or lacking a functional NTRC we have investigated the redundancy and interaction between the NTRC and Fd-TRX systems in regulation of photosynthesis *in vivo*. Overexpression of NTRC raised the CO_2 fixation rate and lowered non-photochemical quenching and acceptor side limitation of PSI in low light conditions by enhancing the activation of chloroplast ATP synthase and TRX-regulated enzymes in Calvin-Benson cycle (CBC). Overexpression of NTRC with an inactivated NTR or TRX domain partly recovered the phenotype of knockout plants, suggesting crosstalk between the plastid TRX systems. NTRC interacted *in planta* with fructose-1,6-bisphosphatase, phosphoribulokinase and $CF_1\gamma$ subunit of the ATP synthase as well as with several chloroplast TRXs. These findings indicate that NTRC-mediated regulation of the CBC and ATP synthesis occurs both directly and through interaction with the ferredoxin-TRX system and is crucial when availability of light is limiting photosynthesis.

KEYWORDS: chloroplast, thioredoxins, NTRC, Calvin–Benson cycle, ATP-synthase

INTRODUCTION

Thioredoxins (TRXs) are ubiquitous enzymes in almost all life forms. They regulate a large number of processes in cell compartments by reducing disulphide bridges in their target proteins. Oxidized TRXs are reduced by thioredoxin reductases (TRs), and a TRX and its corresponding TR constitute a TRX system. TRXs are particularly numerous in plants and TRX-mediated thiol modification is a pivotal regulatory element in plant development and in acclimation to fluctuating light conditions and other environmental factors (Buchanan & Balmer 2005, Meyer et al. 2012, Balsera et al. 2014, Nikkanen & Rintamäki 2014). Two types of TRX systems and over twenty TRX isoforms are localized to plant plastids (Meyer et al. 2012). The ferredoxin-dependent TRX system receives reducing power from photosystem I via reduced ferredoxin and ferredoxin-thioredoxin reductase (FTR). FTR mediates redox signals at least via TRXf1, TRXf2, four isoforms of TRXm, TRXx, TRXy1 and TRXy2 (Schürmann & Buchanan 2008). As ferredoxin is mainly reduced in the light reactions of photosynthesis, the ferredoxin-dependent TRX system is responsible for light-induced activation of primary photosynthetic reactions, namely the Calvin-Benson-cycle (CBC) (Michelet et al. 2013, Geigenberger & Fernie 2014), ATP-synthesis (Hisabori et al. 2013), malate-oxaloacetate shuttle (Miginiac-Maslow et al. 2000) and starch metabolism (Thormählen et al. 2013). TRXx, TRXy and CDSP32 mainly function in response to oxidative stress (Collin et al. 2003, Collin et al. 2004, Broin et al. 2002), while TRXz regulates plastidial transcription (Arsova et al. 2010, Bohrer et al. 2012).

The other type of plastidial TRX system is dependent on NADPH as reductant, and comprises of a single enzyme, NADPH-dependent thioredoxin reductase (NTRC). NTRC is of cyanobacterial origin and has both an N-terminal reductase domain and a C-terminal TRX domain. It forms homodimers where the reductase domain of one subunit reduces the disulphide of the TRX

domain of the other subunit (Serrato et al. 2004, Perez-Ruiz & Cejudo 2009). NTRC can also function in the dark as NADPH can be produced independently of light in the oxidative pentose phosphate pathway (Cejudo et al. 2014). The *NTR*C knockout line of Arabidopsis has a strong photoperiod-dependent phenotype of stunted growth and low chlorophyll content, underlining the crucial role of the enzyme in plant development and chloroplast function (Perez-Ruiz et al. 2006, Lepistö et al. 2009, Michalska et al. 2009, Kirchsteiger et al. 2012).

Based on *in vitro* studies and knockout mutants of chloroplast TRs, the NTRC and Fd-TRX systems are proposed to be non-redundant with no crosstalk between the systems (Perez-Ruiz et al. 2006, Schürmann & Buchanan 2008, Bohrer et al. 2012, Wang et al. 2014). The Fd-TRX system has been regarded as an exclusive thiol exchange regulator of Calvin–Benson cycle enzymes, including fructose-1,6-bisphosphatase (FBPase) and sedoheptulose-1,7-bisphosphatase (SBPase), phosphoribulokinase (PRK) and glyceraldehyde-3-phosphate dehydrogenase (GAPDH), with TRXf1 isoform being the primary TRX involved in light-activation of the enzymes (Jacquot et al. 1978, Brandes, Larimer & Hartman 1996, Schürmann & Buchanan 2008, Marri et al. 2009, Michelet et al. 2013). TRXf is also considered to be mostly responsible for the light-induced reduction of the γ subunit of the chloroplast ATP synthase ($CF_1\gamma$) (Schwarz, Schürmann & Strotmann 1997, Hisabori et al. 2013). NTRC, in turn, has been shown to regulate chloroplast carbon metabolism beyond the primary photosynthetic reactions as well as reactive oxygen species (ROS) metabolism (Perez-Ruiz et al. 2006, Lepistö et al. 2009, Michalska et al. 2009, Richter et al. 2013, Lepistö et al. 2013). NTRC and Fd-TRX systems do nonetheless functionally overlap with relation to their target proteins (Nikkanen & Rintamäki 2014, Thormählen et al. 2015). Both systems have been shown to regulate the activity of ADP-glucose pyrophosphorylase in starch biosynthesis (Michalska et al. 2009, Lepistö et al. 2013, Thormählen

et al. 2013), 2-cysteine-peroxiredoxins (2-Cys PRXs) in ROS metabolism (Perez-Ruiz et al. 2006, Bernal-Bayard et al. 2014), and Mg-protoporphyrin methyltransferase in chlorophyll biosynthesis (Luo et al. 2012, Richter et al. 2013). Similarly to NTRC overexpression in Arabidopsis (Toivola et al. 2013), overexpression of TRXf in tobacco increases biomass yield and starch production (Sanz-Barrio et al. 2013). We have shown recently that in addition to wild-type NTRC, overexpression of NTRC with an inactivated thioredoxin domain (TRXd) (OE-SGPS line) in Arabidopsis *NTR*C-knockout background almost completely rescues the stunted phenotype of the *ntrc* mutant (Toivola et al. 2013). This result suggested that the remaining functional reductase domain (NTRd) interacts with free chloroplast TRXs. When the NTRC gene with an inactivated reductase domain (OE-SAIS line) was overexpressed, some recovery of the *ntrc* phenotype in terms of biomass was observed. Such partial recovery suggested that FTR is capable of interacting and reducing the TRX domain of an overexpressed NTRC lacking a functional NTR domain.

In this article we have investigated the redundancy and dynamics of the NTRC and Fd-TRX systems in Arabidopsis illuminated at differing light intensities and the impact of NTRC on the regulation of photosynthesis *in vivo*. We show that NTRC has an impact on activation of redox-regulated photosynthetic enzymes and overexpression of NTRC enhances photosynthetic yield particularly at low light intensity.

MATERIALS AND METHODS

Plant material and growth conditions

Wild type A*rabidopsis thaliana* of the Columbia ecotype (Col-0), T-DNA insertion mutant line of *NTR*C (At2g41680) SALK_096776 (Alonso et al. 2003, Lepistö et al. 2009), T2 generation plants of the OE-SAISSGPS lines as well as homozygous T3 or T4 generation plants of the OE-NTRC, OE-SAIS and OE-SGPS lines (Toivola et al. 2013) were grown in 1:1 mixture of soil and vermiculate under 100 or 500 µmol of photons m^{-2} s^{-1} at 23°C in a short day (8-h light/16-h dark) photoperiod. Experimental details are provided in the appropriate figure legends. To generate the OE-SAISSGPS line the OE-SAIS.pGWR8 construct (Toivola et al. 2013) was used as a template in mutagenesis by Quickchange XL Site-Directed Mutagenesis kit (Agilent, Santa Clara, CA, USA) to introduce C454S and C457S mutations in the *NTR*C coding sequence. The construct was then sequenced and subsequently introduced to A*grobacterium tumefaciens* strain GV3101 by electroporation. Floral dipping (Clough & Bent 1998) was then used to transform the *ntrc*-knockout line of A*rabidopsis* (SALK_096776) with the construct. T0 and subsequently T1 and T2 seeds were selected on 0.8% agar plates with 0.5x Murashige and Skoog basal salt mixture (Sigma-Aldrich, St Louis, MO, USA) with 50 µg/ml of kanamycin. Overexpression was confirmed by immunoblotting with an NTRC-specific antibody as described below. Wild type *Nicotiana benthamiana* plants for bimolecular fluorescence complementation (BiFC) tests were grown under 130 µmol photons $m^{-2}s^{-1}$ at 23°C in a long day (16-h light/8-h dark) photoperiod.

Measurements of chlorophyll fluorescence, P700 oxidation and ECS decay kinetics

Chl fluorescence and P700 oxidation level were measured with the pulse-amplitude-modulated fluorometer Dual-PAM-100 (Heinz Walz GmbH, Effeltrich, Germany) from detached mature leaves of 5-weeks-old plants grown under 500 µmol photons $m^{-2}s^{-1}$ at 23°C in a short day

photoperiod. A saturating pulse induction curve program with actinic light (AL) of 38 µmol photons $m^{-2}s^{-1}$ for 450 s or a saturating pulse light curve program with AL of 0, 10, 17, 26, 57 and 99 µmol photons $m^{-2}s^{-1}$ for 90 s, and with AL of 130, 220, 343, 535, 829, 1291 and 1958 µmol photons $m^{-2}s^{-1}$ for 30 s was carried out to simultaneously determine the Chl fluorescence and P700 oxidation from dark-adapted (10 min) leaves. The photosynthetic parameters were calculated with the DualPAM software using equations outlined in (Kramer et al. 2004) and (Klughammer & Schreiber 1994). Activation state of the chloroplast ATP synthase was determined with the Dual-PAM-100 fluorometer by measuring the flash-induced absorbance changes at 520 nm known as the electrochromic shift (ECS), which is indicative of changes in the proton motive force (pmf) over the thylakoid membrane (Kramer & Crofts 1989, Kanazawa & Kramer 2002, Kohzuma et al. 2013). The extent of the rapid phase of ECS decay is dependent on the conductivity of the ATP synthase (Kramer & Crofts 1989). Dark-adapted leaves were kept in darkness for 15 min prior to administering a non-saturating light pulse of 100 µs. Measurements were repeated five to six times and representative curves are presented in the article.

CO_2 assimilation measurements

CO_2 fixation was measured from attached mature leaves of 5–6 week-old plants grown under 500 µmol photons $m^{-2}s^{-1}$ at 23°C in a short day photoperiod using a LI-6400 XT portable photosynthesis system (LI-COR, Lincoln, NE, USA). The measurements were conducted with a block temperature of 23°C, 50–60% relative humidity, and a CO_2 concentration of 400 ppm. The light response curves were obtained by measuring CO_2 fixation at 0, 25, 50, 75, 100, 150, 200, 400, 600, 800 and 1000 µmol photons $m^{-2}s^{-1}$. The results were fitted to the model $P_N = (I \times P_{MAX})$

157 / ($I + I_{50}$) – R_D described by (Kaipiainen 2009) and a Microsoft Excel spreadsheet template from
158 (Lobo et al. 2014) was used to calculate the CO_2 fixation parameters.

159

160 **BiFC tests**

161 Full-length coding sequences of NTRC, $NTRC_{SAIS}$ (Toivola et al. 2013), $NTRC_{SGPS}$ (Toivola et
162 al. 2013), TRXf1, TRXf2, TRXm1, TRXm2, TRXm3, TRXm4, TRXx, TRXy1, TRXy2, TRXz,
163 FTRc, CF1γ, PRK and FBPase were cloned into pSPYNE-35S and pSPYCE-35S binary BiFC
164 vectors carrying the N and C-terminal fragment of YFP, respectively (Walter et al. 2004) using
165 appropriate restriction enzymes (Supporting Information Table S1) and checked by sequencing.
166 Cells of A*grobacterium tumefaciens* strain GV3101 were transformed with these plasmids along
167 with the p19 silencing suppressor plasmid (Voinnet et al. 2003) by electroporation. Transformed
168 agrobacterium cells were selected by growing for two days at 28°C on LB agar plates with 35
169 μg/ml of rifampicin, 50 μg/ml of gentamicin sulphate and 50 μg/ml of kanamycin, grown in
170 liquid LB with the same antibiotics overnight and co-infiltrated with p19 into WT *Nicotiana*
171 *benthamiana* leaves according to (Waadt & Kudla 2008). YFP-fluorescence indicative of protein
172 interaction in discs of infiltrated leaves was imaged with a Zeiss LSM510 META laser scanning
173 confocal microscope (Jena, Germany) 2–5 days after infiltration.

174

175 **Protein extraction, SDS-PAGE and Western blotting**

176 Leaf proteins were extracted and thylakoids isolated as described previously (Lepistö et al. 2009,
177 Toivola et al. 2013). The protein content of soluble extracts was determined with the Bio-Rad

Protein Assay Kit (Bio-Rad Laboratories, Hercules, CA, USA) and chlorophyll content of thylakoids according to (Porra, Thompson & Kriedemann 1989). Protein samples were solubilised in Laemmli's buffer (Laemmli 1970) and heated at 100°C for 2 min (soluble proteins) or at 65°C for 5 min (thylakoids) prior to SDS-PAGE. Optimized amounts of proteins for each antibody were separated on 12% or 15% polyacrylamide gels containing 6M urea and blotted on PVDF membranes (Merck Millipore, MA, USA). Membranes were blocked for 2 h with 4% milk in TTBS and subsequently probed overnight at 4°C with a primary antibody raised against PRK (Agrisera AB, Vännas, Sweden, AS07 257), FBPase (kindly provided by Dr. M. Sahrawy, CSIC, Spain), CF1γ (Agrisera, AS08 312), 2-Cys PRXs (kindly provided by prof. F.J. Cejudo, Institute of Plant Biochemistry, University of Sevilla), TRXf1/2 (Agrisera, AS14 2808) or NTRC (Lepistö et al. 2009). An HRP-conjugated goat-anti-rabbit secondary antibody (Agrisera, AS09 602) was applied for 2–4 h. All immunoblots shown are representative of at least three biological replicates of similar results. Protein quantifications from blots were performed with the ImageJ software (Schneider, Rasband & Eliceiri 2012).

Co-immunoprecipitation

The Pierce Co-IP kit (Thermo Fisher Scientific, Rockford, IL USA) was used for the co-immunoprecipitation (co-IP) assays following the manufacturer's instructions unless specified otherwise. 100 mg of OE-NTRC or *ntrc* leaf material was ground in liquid nitrogen and lysed in IP Lysis/Washing Buffer (Pierce). NTRC antibody (Lepistö et al. 2009) was affinity purified in a Protein A Sepharose (CL-4B, GE Healthcare, Waukesha, WI, USA) and covalently immobilized in the AminoLink Plus Resin (Pierce). Leaf lysate containing 1 mg of protein was incubated

overnight at 4°C in the NTRC antibody–containing resin. The resin was washed seven times with IP Lysis/Washing Buffer and proteins bound to the column were eluted with the Pierce elution buffer, pH 2.8. Eluate was then desalted with Modified Dulbecco`s PBS (Pierce), concentrated using an Amicon Ultracentrifugal 3k filter, and the protein content of lysate, final washing sample and eluate determined with the Bio-Rad Protein Assay Kit prior to SDS-PAGE. Two µg of proteins from the lysates and OE-NTRC eluate samples were loaded on the SDS-gels. The protein content of the washing samples and *ntrc* eluate was under the detection limit, hence 50 µl of those solutions were loaded on gels. SDS-Gels were either stained with SYPRO Ruby Protein Gel Stain (Thermo Fisher Scientific) or blotted and probed with appropriate antibodies as described above.

Alkylation of protein thiols

TCA precipitation and MAL-PEG labelling were performed according to the protocol published earlier (Peled-Zehavi, Avital & Danon 2010). 50 mg of leaf material per sample was collected from plants kept under 0, 10, 50, 500 or 1000 µmol of photons $m^{-2}s^{-1}$ for 2 h, ground in 500 µl of 10% trichloroacetic acid (TCA), kept on ice for 20 min and centrifuged at 14000 g for 20 min at 4°C. The pellets were washed with 80% acetone in 50 mM Tris-HCl pH 7.0. Centrifugation and acetone wash were repeated 2 times, last time with 100 % acetone. Pellets were dried and resuspended in a denaturing buffer containing 8 M urea, 100 mM Tris-HCl (pH 7.5), 1 mM EDTA, 2% (w=v) SDS, 1:10 of protease inhibitor cocktail (Thermo Scientific) and 50 mM N-ethylmaleimide (NEM) (Sigma-Aldrich). NEM blocks free thiols with only a slight increase of molecular weight. Samples were then incubated for 30 min at RT, after which 100 mM DTT was

added to experimental samples to reduce *in vivo* disulphide bonds and those samples were incubated for 30 min at room temperature (RT). TCA precipitation and acetone-washing of the samples were repeated, after which all samples were resuspended in denaturing buffer with 10 mM of methoxypolyethylene glycol maleimide M_n=5000 (MAL-PEG) (Sigma-Aldrich) and incubated for 2 h at 27°C. MAL-PEG binds to free thiols in proteins, increasing the molecular mass of the protein by 5 kDa per MAL-PEG bound. The mass increase from a single reduced disulphide is therefore 10 kDa, but due to extensive hydration of PEG, the mobility shift in SDS-PAGE can be much larger, up to 22 kDa per MAL-PEG bound (Makmura et al. 2001, Peled-Zehavi, Avital & Danon 2010). Sample buffer (50mM Tris-HCl, pH 6.8, 2% (w=v) SDS, 10% glycerol, 0.1% bromophenol blue) was added to the samples before SDS-PAGE and Western blotting, which were performed as described above. For thiol-alkylation with 4-Acetamido-4'-Maleimidylstilbene-2,2'-Disulfonic Acid (AMS) (Motohashi et al., 2001), proteins were TCA-precipitated and acetone-washed as above, incubated with 10 mM AMS (Sigma-Aldrich) for 2 h in RT and separated by non-reducing SDS-PAGE. As thiols were not blocked prior to incubation with AMS, the *in vivo* reduced form becomes labelled with AMS and migrates slower in SDS-PAGE.

RESULTS

Phenotypes of plants overexpressing wild type and redox-inactive forms of NTRC

Previously we have shown that overexpression of the *NTR*C gene in *ntrc* mutant background not only fully recovered the stunted low-chlorophyll phenotype of *ntrc*, but also significantly enhanced leaf growth when compared to wild type (Toivola et al. 2013). Partial and substantial recovery of the *ntrc* phenotype was observed when overexpressing *NTR*C with a mutated NTRd

(OE-SAIS) or TRXd (OE-SGPS), respectively. In OE-SAIS and OE-SGPS plants young leaves resembled the chlorotic *ntrc* phenotype, whereas mature leaves showed nearly full recovery of chlorophyll content, especially in the OE-SGPS line (Toivola et al. 2013). In the present study we have constructed homozygous lines overexpressing wild type and mutated NTRC as well as a transgenic line where all the redox active Cys residues in both the NTR and the TRX domain were mutated to serines (OE-SAISSGPS) (Fig. 1). The phenotype of the OE-SAISSGPS line closely resembled that of *ntrc*, indicating that the redox-active cysteines are essential for the function of NTRC *in vivo.* The mutant phenotypes of the *ntrc* knockout and OE-SAIS lines were more prominent when plants where grown in low light than in moderate light (Fig. 1).

The amount of NTRC protein in the overexpression lines was 15 (OE-NTRC), 10 (OE-SAIS), 18 (OE-SGPS) and 7 (OE-SAISSGPS) times higher than in WT (Fig. 1). Since the concentration of NTRC and other TRX proteins are low in comparison to photosynthetic proteins (Peltier et al. 2006, König, Muthuramalingam & Dietz 2012), the amount of NTRC protein in the overexpression lines still remained lower than that of redox-regulated enzymes in the chloroplast. The weaker recovery of the *ntrc* phenotype in the OE-SAIS line when compared to the OE-SGPS line was not due to lower expression level of the NTRC transgene, because an OE-SAIS line that has a higher expression level than the homozygous line used in the experiments of the present study, does not show any better phenotypic recovery (Supporting Information Fig. S1).

Impact of NTRC mutation or overexpression on photosynthetic performance

Since both photosynthetic light reactions and carbon fixation are controlled by chloroplast thiol redox state (Serrato et al. 2013, Balsera et al. 2014), we investigated whether the photosynthetic performance of the NTRC-transgenic lines differs from that of wild type plants. First we measured the light response curves of chlorophyll (Chl) fluorescence and the oxidation level of the reaction center of photosystem I (P700) from detached dark-adapted mature leaves to determine steady-state parameters of light reactions (Fig. 2). The measurements of Chl fluorescence and P700 oxidation indicated that in comparison to WT, the OE-NTRC line had an increased capability to utilize electrons from PSI. PSI yield (YI) was significantly increased (Fig. 2A) and acceptor side limitation of PSI [Y(NA)] decreased (Fig. 2B) in low light intensities. Induction curves with low intensity actinic light (38 μmol photons $m^{-2}s^{-1}$) revealed that in WT Y(NA) is slowly alleviated and Y(I) consequently increased over a measurement of seven minutes, whereas in OE-NTRC Y(NA) was already negligible immediately after dark adaption (Fig. 2E and F). Accordingly, all NTRC-mutated lines (OE-SAIS, OE-SGPS and OE-SAISSGPS) showed an opposite pattern with lower PSI yield (YI) (Fig. 2A) and increased acceptor side limitation of PSI (Y(NA)) (Fig. 2B) in low light intensities. No alleviation of Y(NA) during 7 minutes illumination at low light was observed (Fig. 2E–F). The higher PSII excitation pressure (1-qP) and non-photochemical quenching (NPQ) (Fig. 2C and D) especially in light intensities lower than growth light, also indicated impairment of the linear electron transfer in NTRC-mutated lines. Interestingly, the measured parameters of OE-SGPS were intermediate between WT and OE-SAIS or OE-SAISSGPS lines. The chlorophyll content of the leaves cannot explain the differences observed in chlorophyll fluorescence parameters since no significant differences in the chlorophyll content of mature WT, OE-NTRC, OE-SAIS and OE-SGPS leaves were observed (Toivola et al. 2013).

289

290 Light response curves of CO_2 fixation in transgenic lines were in line with the Chl fluorescence
291 and P700 measurements indicating that deficiency of NTRC impaired and overexpression of
292 NTRC improved photosynthesis under low light intensities (Fig. 3A and B). Both photosynthetic
293 quantum yield of CO_2 assimilation under light intensities limiting photosynthesis and light-
294 saturated CO_2 fixation rate were about 20 % higher in OE-NTRC line in comparison to wild type
295 (Table 1). Light response curve of the OE-SGPS line follows the pattern measured for the OE-
296 NTRC line, whereas OE-SAIS line responded to low light intensities alike previously reported
297 for the *ntrc* mutant (Perez-Ruiz et al. 2006, Lepistö et al. 2009, Pulido et al. 2010). Accordingly,
298 the quantum yield of CO_2 assimilation in OE-SAIS line was substantially reduced under low
299 light, indicating impairment of light utilization capacity in the OE-SAIS line at low light
300 intensity. The results corroborated with the phenotypes of the transgenic lines grown under low
301 light, where the SAIS line produced stunted rosettes resembling *ntrc* line (Fig. 1B). The results
302 also demonstrate the dependency of photosynthetic activity on chloroplast thiol redox state under
303 light intensities limiting photosynthesis. The inability of the OE-SAIS line to use light energy
304 was, however, overcome in higher light intensities. The OE-SAIS line also had higher stomatal
305 conductance and intercellular CO_2 levels than WT or OE-NTRC (Fig. 3C and D), which may
306 partly explain the high steady-state CO_2 assimilation rate of the OE-SAIS line in higher light
307 intensities.

308

309 **NTRC interacts with TRXf1, TRXm1, TRXm3, TRXx, TRXy1 and FTRc *in vivo***

The phenotypic recovery observed in the OE-SAIS and OE-SGPS lines and the photosynthetic performance of the OE-SGPS line suggested that NTRC is able to interact with the FTR-dependent chloroplast TRX system, as suggested previously (Toivola et al. 2013). To test the hypothesis *in vivo* we performed bimolecular fluorescence complementation tests (BiFC) between NTRC, $NTRC_{SAIS}$ or $NTRC_{SGPS}$ and free chloroplast TRXs or the catalytic subunit of FTR (FTRc). We utilised the property of NTRC to interact with itself (Toivola et al. 2013) as a positive control and co-expression of NTRC:YFP-N with the NTRC chloroplast target peptide sequence fused to YFP-C as a negative control in the BiFC assays (Supporting Information Fig. S2). A clear YFP fluorescence signal was observed when NTRC fused with the N-terminal part of YFP was co-expressed with TRXf1, TRXm1, TRXm3, TRXy1, TRXx or FTRc fused with the C-terminal part of YFP in 4-week-old tobacco (*Nicotiana benthamiana*) leaves (Fig. 4A). No YFP fluorescence was observed when NTRC was co-expressed with TRXf2, TRXm2, TRXm4, TRXy2 or TRXz. NTRC also interacted with TRXf1 and TRXm1 when the two redox active cysteines in the reductase domain were mutated to serines ($NTRC_{SAIS}$) and with FTRc when the TRX domain of NTRC was similarly mutated ($NTRC_{SGPS}$) (Supporting Information Fig. S2). This indicates that the physical interactions are independent of the formation of a mixed disulphide between the redox active motifs of the TR and TRX. To confirm the BiFC results, we performed co-immunoprecipitation assays (co-IP) with an immobilized NTRC antibody and leaf lysate from OE-NTRC or *ntrc* leaves. The OE-NTRC lysate yielded abundant protein content in the eluate, while no detectable protein was eluted from the *ntrc* lysate, which was used as a negative control (Fig. 5A). In agreement with the BiFC results, TRXf was detected with a specific antibody in the eluate from OE-NTRC but not from *ntrc* samples (Fig. 5D).

To test the physiological significance of the interactions between NTRC and free chloroplast TRXs we conducted a mobility shift assay with the thiol-alkylating agent AMS to reveal the *in viv*o redox state of TRXf in our NTRC-transgenic lines (Fig. 4B). In dark-adapted leaves the TRXf pool was almost completely oxidized in WT, *ntrc*, OE-SAIS and OE-SGPS lines, but already partly reduced in OE-NTRC. In low light conditions most TRXf remained oxidized in WT, *ntrc* and OE-SAIS, but was mostly reduced in OE-NTRC and interestingly, substantially reduced also in OE-SGPS, which supports the hypothesis that the functional reductase domain of $NTRC_{SGPS}$ is able to reduce other TRXs. In growth light TRXf was more oxidized in OE-SAIS than in WT or even in *ntrc*. This suggests that overexpressed $NTRC_{SAIS}$ might act as a dominant negative regulator by competing with FTR for binding with TRXf. The protein level of TRXf was unaltered in our lines (Supporting Information Fig. S3). Results from our interaction tests and mobility shift assay suggest that the NTRC and Fd-TRX systems form a much more complex and interconnected regulatory network than has previously been proposed.

Thylakoid ATP synthase is activated in darkness in the OE-NTRC line

The analyses of photosynthetic parameters in NTRC-transgenic lines suggested that an elevated thiol redox state in chloroplasts significantly improved the utilization of light energy in CO_2 fixation, especially under low light intensities. Components of light reactions (ATP synthase), primary carbon reactions (Calvin-Benson cycle) and ROS metabolism are directly regulated by thioredoxin systems. Next we therefore investigated how overexpression or mutation of NTRC affected the activation state of the chloroplast ATP synthase.

The chloroplast ATP synthase is inactive in darkness, while generation of proton motive force (pmf) across the thylakoid membrane by light reactions activates the enzyme. Second level regulation consists of TRX-mediated cleavage of a disulphide bridge in $CF_1\gamma$ subunit of the ATP synthase, which reduces the threshold pmf required for activation (Hisabori et al. 2013). Conversely, rapid oxidation of the redox active thiols in darkness, together with depletion of pmf, contributes to the inactivation of the enzyme and prevents futile ATP hydrolysis in darkness (Konno et al. 2012, Hisabori et al. 2013).

To investigate if NTRC overexpression or deficiency affects light-induced activation of the chloroplast ATP synthase, we analysed the depletion of the thylakoid pmf by measuring the decay of the electrochromic shift signal (ECS) following excitation with a short light pulse in light- or dark-adapted leaves (Kramer & Crofts 1989, Klughammer, Siebke & Schreiber 2013). The extent of the rapid phase of ECS decay is indicative of the conductivity of the ATP synthase (Kramer & Crofts 1989, Kohzuma et al. 2013). Measurements of ECS in detached light-adapted mature leaves from all lines show a rapid decay of ECS, indicating a reduced $CF_1\gamma$ and an active ATP synthase (Fig. 6A). In wild type, dark-adaption for 15 minutes is sufficient to result in oxidation of $CF_1\gamma$ and a slower decay of the ECS signal. Dark-adapted OE-NTRC leaves, in contrast, show no difference in ECS decay when compared to light-adapted leaves, indicating that $CF_1\gamma$ remains reduced in darkness in OE-NTRC plants. Dark-adapted *ntrc* leaves, in contrast, displayed slightly slower ECS decay rates than wild type, indicating slower activation of the ATP-synthase upon dark/light transition. OE-SAIS leaves showed ECS decay kinetics similar to WT, while in SGPS leaves the decay was slightly more rapid than in WT.

We used gel shift assays where free thiols in total protein extract from Arabidopsis leaves were labelled with MAL-PEG before separation with SDS-PAGE to determine the *in vivo* redox state

of $CF_1\gamma$ of ATP synthase in the transgenic lines. Corroborating the ECS decay measurements, almost all $CF_1\gamma$ subunits in darkness were oxidized in WT, *ntrc*, OE-SAIS and OE-SGPS samples, whereas a substantial proportion remained in the reduced form in OE-NTRC samples (Fig. 6B). After two hours in low light conditions (50 μmol of photons $m^{-2}s^{-1}$) only reduced $CF_1\gamma$ subunits were already observed in WT and OE-NTRC lines, while in *ntrc*, OE-SAIS and OE-SGPS plants most of the them were oxidized. Even after 2 hours in growth light (500 μmol photons $m^{-2}s^{-1}$) or high light (1000 μmol photons $m^{-2}s^{-1}$) conditions a small proportion of $CF_1\gamma$ subunits remained oxidized in *ntrc*, OE-SAIS and OE-SGPS samples (Fig. 6B). No differences in $CF_1\gamma$ protein level were observed between the transgenic lines and WT (Supporting Information Fig. S3).

Both the ECS decay kinetics and thiol labelling of ATP synthase results suggested a direct involvement of NTRC in regulation of the activation state of the ATP synthase. Indeed, BiFC assays showed that $CF_1\gamma$ directly interacts with both NTRC and TRXf1, but not with TRXx. The $CF_1\gamma$-NTRC interaction was also confirmed with co-IP (Fig. 5E).

Redox status of TRX-regulated enzymes in the Calvin–Benson cycle

The quantum yield and light-response curve of CO_2 assimilation indicated that changes in the chloroplast thiol redox state modified primary carbon metabolic pathways in transgenic NTRC lines. We used MAL-PEG labelling to determine the *in vivo* redox state of TRX-regulated CBC enzymes phosphoribulokinase (PRK) and fructose-1,6-bisphosphatase (FBPase) (Michelet et al. 2013) in our transgenic lines. FBPase and PRK were oxidized in darkness in WT, while light induced partial reduction of both enzyme pools (Fig. 7A). Only oxidized forms of FBPase and

PRK appeared to be present in *ntrc*, OE-SAIS and OE-SGPS lines in darkness and low light (50 μmol of photons $m^{-2}s^{-1}$) and only a minor proportion of the enzyme pools became reduced under 500 and 1000 μmol photons $m^{-2}s^{-1}$. The proportion of reduced form of FBPase and PRK was higher in the OE-NTRC line than in WT in darkness and in all light conditions tested. There were no differences in protein levels of PRK or FBPase between the transgenic lines and WT (Supporting Information Fig. S3). Higher and lower photosynthetic quantum yields of the OE-NTRC and OE-SAIS lines, respectively, at low light intensities (Fig. 2, Table 1) might therefore be at least partly caused by altered redox states of CBC enzymes.

The considerably higher proportions of oxidized forms of PRK and FBPase *in vivo* in *ntrc*, OE-SAIS and OE-SGPS lines when compared to WT in all light intensities provided further indication of direct involvement of NTRC in thiol-exchange activation of the Calvin–Benson cycle. In order to test this hypothesis, we performed BiFC assays between PRK or FBPase and NTRC, TRXf1 and TRXx. Our results show that both PRK and FBPase interacted *in planta* with NTRC and TRXf1 but not with TRXx (Fig. 7B). The NTRC-FBPase and NTRC-PRK interactions were further confirmed by co-IP (Fig. 5F).

The effect of overexpression of wild type and mutated NTRC on the redox state of 2-Cys PRXs

The high amount of oxidized PRK and FBPase forms in OE-SAIS and OE-SGPS seemed to contradict, particularly in case of OE-SGPS, the recovery of carbon assimilation capacity of these transgenic lines (Fig. 3, Table 1). NTRC has been shown to be a primary, non-redundant regulator of 2-Cys PRXs redox state in chloroplasts (Perez-Ruiz et al. 2006, Kirchsteiger et al.

2009, Muthuramalingam et al. 2009, Pulido et al. 2010, Bernal-Bayard et al. 2014), which led us to hypothesize that accumulation of ROS in OE-SAIS and OE-SGPS due to ineffective reduction of 2-Cys PRXs might cause rapid re-oxidation of CBC enzymes after transient redox-activation. We therefore investigated the *in vivo* redox state of 2-Cys PRXs in different light intensities with a thiol labelling gel shift assay (Fig. 7A). A light-dependent pattern was observed in the amounts of oxidized and reduced 2-Cys PRXs in WT incubated in darkness and under various light intensities. The double- and single-disulphide forms (Puerto-Galan et al. 2013) dominated in darkness, whereas in low light the proportion of fully reduced enzyme was increased (Fig. 7A). In the OE-NTRC line, the completely and partially reduced forms dominated in all light conditions, even in darkness. In *ntrc* the 2-Cys PRXs pool was almost completely oxidized in darkness, while a small proportion of partially reduced 2-Cys PRXs was present in OE-SAIS and OE-SGPS lines. In light the partially reduced form of 2-Cys PRXs increased, particularly in the OE-SAIS-line, in which FTR likely mediates reduction of the TRX-domain of $NTRC_{SAIS}$ (Fig. 4). The protein level of 2-Cys PRXs was slightly lower in *ntrc*, OE-SAIS and OE-SGPS than in WT but unaltered in the OE-NTRC line (Supporting Information Fig. S3). These results support previous conclusions (Perez-Ruiz et al. 2006, Muthuramalingam et al. 2009, Pulido et al. 2010, Bernal-Bayard et al. 2014) that NTRC is the primary reductant of 2-Cys PRXs while other chloroplast TRXs have only a minor effect on the redox state of 2-Cys PRXs. Thereby it is likely that the *ntrc*, OE-SAIS, and OE-SGPS lines will suffer more and the OE-NTRC line less from oxidative stress than WT.

DISCUSSION

In the present paper we show an improvement of leaf photosynthetic activity by an elevated chloroplast thiol-redox state through NTRC overexpression, especially at low light intensities. In the OE-NTRC transgenic line the quantum yield of CO_2 fixation was increased, because redox-activated processes, namely ATP synthesis and the Calvin–Benson cycle were activated already at low light intensity (Fig. 3, 6 and 7). The efficient utilization of light energy in CO_2 fixation and rapid activation of the ATP synthase were also revealed by the low acceptor site limitation of PSI [Y(NA)] under low light and by the reduced need to dissipate extra energy via NPQ (Fig. 2). Conversely, the *ntrc* mutant and transgenic lines expressing mutated NTRC exhibited higher Y(NA) in low light as well higher NPQ, as inefficient light-activation of ATP synthesis and carbon fixation induced buildup of transthylakoidal ΔpH. High content of wild-type NTRC in the chloroplast also promoted the activity of the chloroplast antioxidant system by keeping 2-Cys-PRXs reduced independently of light conditions (Fig. 7). Consequently, the OE-NTRC line may rapidly alleviate harmful effects from ROS production at physiological light intensities. These alterations in the regulation of the photosynthetic machinery and ROS metabolism may be crucial factors behind the vitality of this transgenic line. Furthermore, improved photosynthetic activity of mature leaves at low light may partly explain higher biomass production of OE-NTRC lines (Toivola et al. 2013), because the mature leaves become shaded by young leaves in the course of rosette growth. The transgenic lines overexpressing WT and active-site-mutated NTRC also revealed that the chloroplast TRX systems do not only overlap at the level of target proteins but the systems form an interconnected functional redox network that can dynamically respond to changing environmental conditions. NTRC can mediate reducing equivalents through distinct chloroplast TRXs to chloroplast metabolism, while FTR is able to act via the TRXd of NTRC *in*

464 *vivo* (Fig. 8). Our data also supports the idea that the specificity between TRXs and their target
465 proteins relies on surface structures outside redox-active Cys in TRXs.

466

467 **Crosstalk between NTRC and Fd-TRX systems**

468 The recovery of the OE-SGPS and OE-SAIS transgenic lines is indicative of crosstalk between
469 plastidial TRX systems, and indeed the results from our interaction assays show that NTRC
470 interacts with TRXf1, TRXm1, TRXm3, TRXx, TRXy1, and the catalytic subunit of FTR
471 (FTRc) (Fig. 4A). Immunoprecipitation of TRXf with NTRC (Fig. 5) and a high reduction of
472 TRXf pool in OE-NTRC line at low light intensity (Fig. 4B) support both protein-protein and
473 functional interaction of NTRC with TRXf. The conclusions in this article have been drawn from
474 experiments carried out with NTRC overexpression lines. However, a recent publication by
475 Thormählen et al. (2015) supports the interaction between NTRC and TRXf even with wild-type
476 expression levels of chloroplast thioredoxins. They showed that although the *trxf1* knockout line
477 had no visible phenotype, the knockout of both NTRC and TRXf1 substantially impaired growth
478 and photosynthesis in Arabidopsis in comparison to the *ntrc* single mutant line.

479 The lower recovery of the OE-SAIS in comparison to the OE-SGPS line can be explained by
480 negative interference of mutated NTRC with FTR system and/or by FTR content in chloroplast
481 (Fig. 8). The high amount of oxidized TRXf in illuminated OE-SAIS line (Fig. 4B) suggests that
482 overexpressed $NTRC_{SAIS}$ acts as a dominant negative regulator for the FTR system, competing
483 with FTR for binding with TRXf1 and thereby lowering the total reducing capacity of
484 chloroplast TRX systems. Moreover, it has been estimated that the content of chloroplast
485 thioredoxins and NTRC is ten to hundred-fold lower than the content of metabolic enzymes in

chloroplasts (Peltier et al. 2006, König, Muthuramalingam & Dietz 2012). No report on the protein content of FTR in chloroplast is available but the expression level of FTR genes in Arabidopsis leaves is equal to the levels of the genes encoding TRXf and m isoforms (Bohrer et al. 2012, Belin et al. 2015). Hence the low amount of FTR likely limits the reduction of TRXd of NTRC independently of the amount of $NTRC_{SAIS}$ protein.

The colour of young and mature OE-SAIS and OE-SGPS leaves resembled *ntrc* and wild type plants, respectively, suggesting that some of the processes in leaf development and chloroplast biogenesis are primarily regulated by NTRC (Lepistö et al. 2009, Lepistö & Rintamäki 2012), and can only poorly be compensated by Fd-TRX system. Moreover, knockout of *FTRc* is lethal, while virus-induced gene silencing (VIGS) of *FTRc* resulted in chlorotic young leaves with poorly developed chloroplasts (Wang et al. 2014). As those leaves matured, however, a WT-like phenotype was restored, indicating that similarly to the NTRC active-site mutants, the developing chloroplast also has processes non-redundantly regulated by the Fd-FTR system (Wang et al. 2014). In both cases it is likely that the development of chloroplasts in leaves is slowed down, but after reaching a specific developmental threshold, interaction or redundancy between the FTR-TRX and NTRC systems accounts for the recovery of phenotype in mature leaves.

Results from our BiFC assays suggest that NTRC interacts with TRXf1, but not with TRXf2, the amount of which is a third of TRXf1 in Arabidopsis leaves (Okegawa & Motohashi 2015). It has already been shown previously that NTRC can reduce TRXf1 in an *in vitro* assay, albeit inefficiently (Fig. S4 in Bohrer et al., 2012). The NTRC–TRXf1 interaction probably compensates for the lack of a functional TRX domain of NTRC in our OE-SGPS line and thereby explains the recovery of the *ntrc* phenotype (Toivola et al. 2013). Our results verify the

509 suggestion proposed in recent papers (Yoshida, Hara & Hisabori 2015, Thormählen et al. 2015)
510 that cross-talk and redundancy between the NTRC and FTR-TRXf systems plays a role in
511 regulating the CBC and ATP synthase activation, which are the most comprehensively
512 characterized chloroplast processes regulated by TRXf1 (Schürmann & Buchanan 2008).

513 Interestingly, NTRC also interacted with TRXm1, TRXm3, TRXx, and TRXy1, but no
514 interaction was observed with TRXm2, TRXm4, TRXy2 or TRXz (Fig. 4). The m-type TRXs
515 are of prokaryotic origin and were first described as thiol activators of chloroplast NADP-malate
516 dehydrogenase (MDH) (Schürmann & Buchanan 2008). TRXm1 and m2 have been proposed to
517 have roles as secondary thiol regulators of the CBC, having lower activation capabilities of CBC
518 enzymes than TRXf (Wolosiuk et al. 1979, Michelet et al. 2013), albeit opposite results about the
519 role of TRXf and TRXm in the regulation of photosynthesis have recently been published
520 (Okegawa & Motohashi 2015). TRXm4 has been suggested to be involved in regulation of
521 alternative photosynthetic electron transfer pathways (Courteille et al. 2013) and TRXm1, m2
522 and m4 in biogenesis of photosystem II (Wang et al. 2013). Overexpression of TRXm, in
523 contrast to OE of TRXf (Sanz-Barrio et al. 2013) or NTRC (Toivola et al. 2013), reduces growth,
524 photosynthetic activity and chlorophyll content of tobacco while increasing tolerance of
525 oxidative stress (Rey et al. 2013). TRXm3 and TRXy1 have been suggested to regulate
526 development of symplastic permeability and activity of monodehydroascorbate reductase in the
527 glutathione–ascorbate cycle, respectively (Benitez-Alfonso et al. 2009, Marchand et al. 2010).
528 The potential role of NTRC in these processes regulated by TRXm and TRXy isoforms remains
529 to be elucidated in future studies.

530 The OE-SAISSGPS line, where both NTR and TRX domains of NTRC are inactivated, shows
531 only minor signs of recovering the *ntrc* phenotype (Fig. 1). It has been suggested that NTRC also

has foldase and holdase chaperone functions under heat shock with the foldase activity being redox-dependent and holdase activity independent of the reductase and TRX activities of NTRC (Chae et al. 2013). $NTRC_{SAISSGPS}$ might therefore still be able to elicit a holdase chaperone function, but it does not seem to be sufficient to substantially recover the *ntrc* phenotype of OE-SAISSGPS under the growth conditions studied in this paper.

NTRC regulates the activity of the chloroplast ATP synthase through reduction of the γ subunit

Activation state of the chloroplast ATP synthase is regulated by proton motive force (pmf) formed by the photosynthetic electron transfer reactions and by reduction of a disulphide in the γ subunit ($CF_1\gamma$) by TRX (Hisabori et al. 2013, Kohzuma et al. 2013). ECS decay kinetics and the partly reduced *in vivo* redox state of $CF_1\gamma$ (Fig. 6) in dark-adapted leaves of the OE-NTRC line indicate that a proportion of the $CF_1\gamma$ pool remains reduced in darkness in OE-NTRC plants. Since we also demonstrated that NTRC interacts with $CF_1\gamma$ *in planta* (Fig. 5 and 6C) and that $CF_1\gamma$ remains oxidized in low light in *ntrc* and transgenic plants expressing mutated NTRC (Fig. 6B), we propose that NTRC is involved in the regulation of ATP synthase activation *in vivo*, and is particularly important in low light conditions. Overexpression of NTRC likely results in activation of the chloroplast ATP synthase in darkness, and as the pmf across the thylakoid membrane is depleted in darkness, a dark-activated ATP synthase will likely exhibit reverse activity; wasteful pumping of protons back to the lumen powered by hydrolysis of ATP to ADP and P_i. In this regard, the OE-NTRC line may resemble the redox-insensitive *mothra* mutant line

553 of $CF_1\gamma$ (Kohzuma et al. 2013). However, this futile activation of ATP synthase affects neither
554 the phenotype nor growth of the OE-NTRC line (Fig. 1) (Toivola et al. 2013).

555 Interestingly, *trxf1-trxf2* double mutants show no impairment in light-dependent reduction of
556 $CF_1\gamma$ (Yoshida, Hara & Hisabori 2015), while in *ntrc,* OE-SAIS and OE-SGPS the $CF_1\gamma$ pool is
557 inefficiently reduced in low light when compared to WT, but reaches full reduction in higher
558 light intensities (Fig. 6B). This suggests that while both TRXf1 and NTRC interact with $CF_1\gamma$
559 (Fig. 6C), NTRC has a primary role in activation of the ATP synthase. We propose that NTRC is
560 required for effective reduction of $CF_1\gamma$ in low light, while the FTR-TRXf1 system is able to
561 compensate for a lack of NTRC in higher light intensity.

562

563 **Crosstalk between NTRC and Fd-FTR systems in regulation of CO_2 assimilation**

564 In the present paper we show that the proportions of redox-activated form of FBPase, and
565 especially that of PRK were higher in the OE-NTRC line but lower in *ntrc*, OE-SAIS and OE-
566 SGPS plants (Fig. 7A) when compared to WT, pointing to direct participation of NTRC in
567 regulation of the CBC. Direct interaction of NTRC with PRK and FBPase *in planta* supports this
568 conclusion (Fig. 5 and 7B). Accordingly, Yoshida and colleagues showed recently (Yoshida,
569 Hara & Hisabori 2015) that the redox states of FBPase and SBPase as well as overall plant
570 phenotype were almost unaffected both in a *trxf1* mutant and a *trxf1 trxf2* double mutant. That
571 may at least partly be explained by the activation of CBC enzymes by TRXm1 and TRXm2, as
572 suggested recently (Okegawa & Motohashi 2015). We showed that NTRC interacts with TRXm1
573 (Fig. 4A), suggesting that TRXm1 may also account for the phenotypic recovery of the OE-
574 SGPS line. Cross-talk and redundancy between NTRC, TRXf1 and TRXm1 may provide a way

to fine tune the activity of the CBC in response to changes in environmental conditions that affect the chloroplast redox state or induce production of ROS. We propose that NTRC-mediated reduction would be physiologically important in activating CBC enzymes in low light conditions, and that the Fd-TRX system would require higher light intensity to effectively maintain CBC activity.

The drastically oxidized redox states of PRK and FBPase in OE-SAIS and OE-SGPS (Fig. 7A) first seemed to contradict our measurements of CO_2 assimilation rates in those lines (Fig. 3). This discrepancy might be explained by ROS metabolism (Fig. 8). We showed that oxidized forms of 2-Cys PRXs dominate in chloroplasts of *ntrc*, OE-SAIS and OE-SGPS lines (Fig. 7A), suggesting increased accumulation of ROS in all studied light conditions. Pulido et al. (Pulido et al. 2010) reported a 30 % increase in accumulation of H_2O_2 in *ntrc* mutant leaves in comparison to WT. High accumulation of reduced 2-Cys PRX forms in OE-NTRC line and of the oxidized form in *ntrc*, OE-SAIS and OE-SGPS lines supports the primary role of NTRC in reduction of 2-Cys PRXs in chloroplasts, as suggested earlier (Pulido et al. 2010). The oxidative redox state in *ntrc*, OE-SAIS and OE-SGPS chloroplasts likely accelerates the oxidation of redox-regulated CBC enzymes resulting in steady-state accumulation of the oxidized forms of the enzymes. The capacity to recover the active enzyme depends on the availability of reductants, which is higher in the OE-SGPS line than in *ntrc* (NTRC is missing) or the OE-SAIS line (negative interference of mutated NTRC with the FTR system) (Fig. 8). The higher reducing capacity in OE-SGPS chloroplasts enables a CO_2 fixation rate (Fig. 3) and recovery of phenotype (Fig. 1) comparable to WT.

The well-established role of the Fd-TRX system is to connect light and carbon fixation reactions by activating CBC enzymes in dark-light transition (Schürmann & Buchanan 2008, Michelet et

al. 2013). NTRC can be reduced both by NADPH generated in the oxidative pentose phosphate pathway (OPPP) in darkness and by light reactions in light, prompting a question about futile activation of CBC enzymes in darkness in the OE-NTRC lines. Nevertheless, overexpression of *NTRC* increased instead of impairing biomass production (Toivola et al. 2013), suggesting that the putative negative consequences of partial dark-activation of photosynthetic reactions were at least outweighed by the positive effect of increased TRX reducing capacity. Moreover, the amounts of reduced CBC enzymes in darkness were only modestly raised (Fig. 7A). This is likely due to the multiple mechanisms that regulate the photosynthetic enzymes *in vivo*. In addition to activation of TRXs, illumination changes pH and ion concentrations in stroma and lumen, concentrations of the substrates and availability of cofactors, all of which influence the steady-state activity of the ATP synthase and CBC enzymes (Stitt, Lunn & Usadel 2010, Kohzuma et al. 2013, Hochmal et al. 2015). Multiple levels of regulation allow fine-tuning of photosynthesis in fluctuating environmental conditions.

Conclusions

In the paper we have investigated the redundancy and dynamics between the ferredoxin- (FTR) and NADPH-dependent (NTRC) thioredoxin systems in photosynthesis *in vivo*. We show that the two chloroplast TRX systems form an interconnected functional redox network that can dynamically respond to changing light conditions and thus improve plant fitness. It is also demonstrated that an elevated chloroplast thiol-redox state through NTRC overexpression improves leaf photosynthetic activity and that in addition to FTR, NTRC system participates in

regulation of primary photosynthetic reactions and is particularly important in conditions where light limits photosynthesis.

ACKNOWLEDGEMENTS

We thank Drs. F.J Cejudo and M. Sahrawy for donation of antibodies, M. Rahikainen for the $CF_1\gamma$ BiFC construct, A. Lepistö and J. Sulku for assistance in the experiments, Dr. M. Keränen and K. Ståhle for technical assistance as well as Dr. M. Nurmi for invaluable advice. This work was funded by Academy of Finland Grants 276392 and 271832 (the Center of Excellence in Molecular Biology of Primary Producers) and by the Doctoral Program in Molecular Life Sciences in the University of Turku Graduate School.

REFERENCES

Alonso J.M., Stepanova A.N., Leisse T.J., Kim C.J., Chen H.M., Shinn P., ..., Ecker J.R. (2003) Genome-wide insertional mutagenesis of arabidopsis thaliana. *Science* **301,** 653-657.

638 Arsova B., Hoja U., Wimmelbacher M., Greiner E., Ustun S., Melzer M., ..., Boernke F. (2010)
639 Plastidial thioredoxin z interacts with two fructokinase-like proteins in a thiol-dependent
640 manner: Evidence for an essential role in chloroplast development in arabidopsis and
641 nicotiana benthamiana. *Plant Cell* **22,** 1498-1515.

642 Balsera M., Uberegui E., Schürmann P. & Buchanan B.B. (2014) Evolutionary development of
643 redox regulation in chloroplasts. *Antioxidants & Redox Signaling* **21,** 1327-1355.

644 Belin C., Bashandy T., Cela J., Delorme-Hinoux V., Riondet C. & Reichheld J.P. (2015) A
645 comprehensive study of thiol reduction gene expression under stress conditions in
646 arabidopsis thaliana. *Plant, Cell & Environment* **38,** 299-314.

647 Benitez-Alfonso Y., Cilia M., Roman A.S., Thomas C., Maule A., Hearn S., ..., Jackson D.
648 (2009) Control of arabidopsis meristem development by thioredoxin-dependent regulation of
649 intercellular transport. *Proceedings of the National Academy of Sciences of the United States*
650 *of America* **106,** 3615-3620.

651 Bernal-Bayard P., Ojeda V., Hervas M., Cejudo F.J., Navarro J.A., Velazquez-Campoy A., ...,
652 Perez-Ruiz J.M. (2014) Molecular recognition in the interaction of chloroplast 2-cys
653 peroxiredoxin with NADPH-thioredoxin reductase C (NTRC) and thioredoxin x. *FEBS*
654 *Letters* **588,** 4342-4347.

655 Bohrer A., Massot V., Innocenti G., Reichheld J., Issakidis-Bourguet E. & Vanacker H. (2012)
656 New insights into the reduction systems of plastidial thioredoxins point out the unique
657 properties of thioredoxin z from arabidopsis. *Journal of Experimental Botany* **63,** 6315-6323.

Brandes H.K., Larimer F.W. & Hartman F.C. (1996) The molecular pathway for the regulation of phosphoribulokinase by thioredoxin f. *Journal of Biological Chemistry* **271,** 3333-3335.

Broin M., Cuine S., Eymery F. & Rey P. (2002) The plastidic 2-cysteine peroxiredoxin is a target for a thioredoxin involved in the protection of the photosynthetic apparatus against oxidative damage. *Plant Cell* **14,** 1417-1432.

Buchanan B.B. & Balmer Y. (2005) Redox regulation: A broadening horizon. *Annual Review of Plant Biology* **56,** 187-220.

Cejudo F.J., Meyer A.J., Reichheld J., Rouhier N. & Traverso J.A. (2014) Thiol-based redox homeostasis and signaling. *Frontiers in Plant Science* **5,** 266.

Chae H.B., Moon J.C., Shin M.R., Chi Y.H., Jung Y.J., Lee S.Y., ..., Lee S.Y. (2013) Thioredoxin reductase type C (NTRC) orchestrates enhanced thermotolerance to arabidopsis by its redox-dependent holdase chaperone function. *Molecular Plant* **6,** 323-336.

Clough S. & Bent A. (1998) Floral dip: A simplified method for agrobacterium-mediated transformation of arabidopsis thaliana. *Plant Journal* **16,** 735-743.

Collin V., Issakidis-Bourguet E., Marchand C., Hirasawa M., Lancelin J., Knaff D., ..., Miginiac-Maslow M. (2003) The arabidopsis plastidial thioredoxins - new functions and new insights into specificity. *Journal of Biological Chemistry* **278,** 23747-23752.

Collin V., Lamkemeyer P., Miginiac-Maslow M., Hirasawa M., Knaff D.B., Dietz K.J., ..., Issakidis-Bourguet E. (2004) Characterization of plastidial thioredoxins from arabidopsis belonging to the new y-type. *Plant Physiology* **136,** 4088-4095.

678 Courteille A., Vesa S., Sanz-Barrio R., Cazale A., Becuwe-Linka N., Farran I., ..., Rumeau D.
679 (2013) Thioredoxin m4 controls photosynthetic alternative electron pathways in arabidopsis.
680 *Plant Physiology* **161,** 508-520.

681 Geigenberger P. & Fernie A.R. (2014) Metabolic control of redox and redox control of
682 metabolism in plants. *Antioxidants & Redox Signaling* **21,** 1389-1421.

683 Hisabori T., Sunamura E., Kim Y. & Konno H. (2013) The chloroplast ATP synthase features
684 the characteristic redox regulation machinery. *Antioxidants & Redox Signaling* **19,** 1846-
685 1854.

686 Hochmal A.K., Schulze S., Trompelt K. & Hippler M. (2015) Calcium-dependent regulation of
687 photosynthesis. *Biochimica Et Biophysica Acta-Bioenergetics* **1847,** 993-1003.

688 Jacquot J., Vidal J., Gadal P. & Schürmann P. (1978) Evidence for existence of several enzyme-
689 specific thioredoxins in plants. *FEBS Letters* **96,** 243-246.

690 Kaipiainen E.L. (2009) Parameters of photosynthesis light curve in salix dasyclados and their
691 changes during the growth season. *Russian Journal of Plant Physiology* **56,** 445-453.

692 Kanazawa A. & Kramer D.M. (2002) In vivo modulation of nonphotochemical exciton
693 quenching (NPQ) by regulation of the chloroplast ATP synthase. *Proceedings of the*
694 *National Academy of Sciences of the United States of America* **99,** 12789-12794.

695 Kirchsteiger K., Ferrandez J., Belen Pascual M., Gonzalez M. & Javier Cejudo F. (2012)
696 NADPH thioredoxin reductase C is localized in plastids of photosynthetic and

nonphotosynthetic tissues and is involved in lateral root formation in arabidopsis. *Plant Cell* **24,** 1534-1548.

Kirchsteiger K., Pulido P., Gonzalez M. & Javier Cejudo F. (2009) NADPH thioredoxin reductase C controls the redox status of chloroplast 2-cys peroxiredoxins in arabidopsis thaliana. *Molecular Plant* **2,** 298-307.

Klughammer C. & Schreiber U. (1994) An improved method, using saturating light-pulses, for the determination of photosystem-I quantum yield via P700+-absorbency changes at 830 nm. *Planta* **192,** 261-268.

Klughammer C., Siebke K. & Schreiber U. (2013) Continuous ECS-indicated recording of the proton-motive charge flux in leaves. *Photosynthesis Research* **117,** 471-487.

Kohzuma K., Dal Bosco C., Meurer J. & Kramer D.M. (2013) Light- and metabolism-related regulation of the chloroplast ATP synthase has distinct mechanisms and functions. *Journal of Biological Chemistry* **288,** 13156-13163.

König J., Muthuramalingam M. & Dietz K. (2012) Mechanisms and dynamics in the thiol/disulfide redox regulatory network: Transmitters, sensors and targets. *Current Opinion in Plant Biology* **15,** 261-268.

Konno H., Nakane T., Yoshida M., Ueoka-Nakanishi H., Hara S. & Hisabori T. (2012) Thiol modulation of the chloroplast ATP synthase is dependent on the energization of thylakoid membranes. *Plant and Cell Physiology* **53,** 626-634.

716 Kramer D.M. & Crofts A.R. (1989) Activation of the chloroplast ATPase measured by the
717 electrochromic change in leaves of intact plants. *Biochimica Et Biophysica Acta* **976,** 28-41.

718 Kramer D.M., Johnson G., Kiirats O. & Edwards G.E. (2004) New fluorescence parameters for
719 the determination of Q(A) redox state and excitation energy fluxes. *Photosynthesis Research*
720 **79,** 209-218.

721 Laemmli U. (1970) Cleavage of structural proteins during assembly of head of bacteriophage-T4.
722 *Nature* **227,** 680-685.

723 Lepistö A., Kangasjärvi S., Luomala E., Brader G., Sipari N., Keränen M., ..., Rintamäki E.
724 (2009) Chloroplast NADPH-thioredoxin reductase interacts with photoperiodic development
725 in arabidopsis. *Plant Physiology* **149,** 1261-1276.

726 Lepistö A., Pakula E., Toivola J., Krieger-Liszkay A., Vignols F. & Rintamäki E. (2013)
727 Deletion of chloroplast NADPH-dependent thioredoxin reductase results in inability to
728 regulate starch synthesis and causes stunted growth under short-day photoperiods. *Journal of*
729 *Experimental Botany* **64,** 3843-3854.

730 Lepistö A. & Rintamäki E. (2012) Coordination of plastid and light signaling pathways upon
731 development of arabidopsis leaves under various photoperiods. *Molecular Plant* **5,** 799-816.

732 Lobo F.d.A., de Barros M.P., Dalmagro H.J., Dalmolin A.C., Pereira W.E., de Souza E.C., ...,
733 Rodriguez Ortiz C.E. (2014) Fitting net photosynthetic light-response curves with microsoft
734 excel - a critical look at the models (vol 53, pg 445, 2013). *Photosynthetica* **52,** 479-480.

735 Luo T., Fan T., Liu Y., Rothbart M., Yu J., Zhou S., ..., Luo M. (2012) Thioredoxin redox
736 regulates ATPase activity of magnesium chelatase CHLI subunit and modulates redox-
737 mediated signaling in tetrapyrrole biosynthesis and homeostasis of reactive oxygen species
738 in pea plants. *Plant Physiology* **159,** 118-130.

739 Makmura L., Hamann M., Areopagita A., Furuta S., Munoz A. & Momand J. (2001)
740 Development of a sensitive assay to detect reversibly oxidized protein cysteine sulfhydryl
741 groups. *Antioxidants & Redox Signaling* **3,** 1105-1118.

742 Marchand C.H., Vanacker H., Collin V., Issakidis-Bourguet E., Le Marechall P. & Decottignies
743 P. (2010) Thioredoxin targets in arabidopsis roots. *Proteomics* **10,** 2418-2428.

744 Marri L., Zaffagnini M., Collin V., Issakidis-Bourguet E., Lemaire S.D., Pupillo P., ..., Trost P.
745 (2009) Prompt and easy activation by specific thioredoxins of calvin cycle enzymes of
746 arabidopsis thaliana associated in the GAPDH/CP12/PRK supramolecular complex.
747 *Molecular Plant* **2,** 259-269.

748 Meyer Y., Belin C., Delorme-Hinoux V., Reichheld J. & Riondet C. (2012) Thioredoxin and
749 glutaredoxin systems in plants: Molecular mechanisms, crosstalks, and functional
750 significance. *Antioxidants & Redox Signaling* **17,** 1124-1160.

751 Michalska J., Zauber H., Buchanan B.B., Cejudo F.J. & Geigenberger P. (2009) NTRC links
752 built-in thioredoxin to light and sucrose in regulating starch synthesis in chloroplasts and
753 amyloplasts. *Proceedings of the National Academy of Sciences of the United States of*
754 *America* **106,** 9908-9913.

Michelet L., Zaffagnini M., Morisse S., Sparla F., Perez-Perez M.E., Francia F., ..., Lemaire S.D. (2013) Redox regulation of the calvin-benson cycle: Something old, something new. *Frontiers in Plant Science* **4,** 470.

Miginiac-Maslow M., Johansson K., Ruelland E., Issakidis-Bourguet E., Schepens I., Goyer A., ..., Decottignies P. (2000) Light-activation of NADP-malate dehydrogenase: A highly controlled process for an optimized function. *Physiologia Plantarum* **110,** 322-329.

Motohashi K., Kondoh A., Stumpp M.T. & Hisabori T. (2001) Comprehensive survey of proteins targeted by chloroplast thioredoxin. *Proceedings of the National Academy of Sciences of the United States of America* **98,** 11224-11229.

Muthuramalingam M., Seidel T., Laxa M., de Miranda S.M.N., Gaertner F., Stroeher E., ..., Dietz K. (2009) Multiple redox and non-redox interactions define 2-cys peroxiredoxin as a regulatory hub in the chloroplast. *Molecular Plant* **2,** 1273-1288.

Nikkanen L. & Rintamäki E. (2014) Thioredoxin-dependent regulatory networks in chloroplasts under fluctuating light conditions. *Philosophical Transactions of the Royal Society B-Biological Sciences* **369,** 20130224.

Okegawa Y. & Motohashi K. (2015) Chloroplastic thioredoxin m functions as a major regulator of calvin cycle enzymes during photosynthesis in vivo. *The Plant Journal : For Cell and Molecular Biology*.

Peled-Zehavi H., Avital S. & Danon A. (2010) Methods of redox signaling by plant thioredoxins. pp. 256.

775 Peltier J.B., Cai Y., Sun Q., Zabrouskov V., Giacomelli L., Rudella A., ..., van Wijk K.J. (2006)
776 The oligomeric stromal proteome of arabidopsis thaliana chloroplasts. *Molecular & Cellular*
777 *Proteomics* **5,** 114-133.

778 Perez-Ruiz J.M. & Cejudo F.J. (2009) A proposed reaction mechanism for rice NADPH
779 thioredoxin reductase C, an enzyme with protein disulfide reductase activity. *FEBS Letters*
780 **583,** 1399-1402.

781 Perez-Ruiz J.M., Spinola M.C., Kirchsteiger K., Moreno J., Sahrawy M. & Cejudo F.J. (2006)
782 Rice NTRC is a high-efficiency redox system for chloroplast protection against oxidative
783 damage. *Plant Cell* **18,** 2356-2368.

784 Porra R., Thompson W. & Kriedemann P. (1989) Determination of accurate extinction
785 coefficients and simultaneous-equations for assaying chlorophyll-a and chlorophyll-B
786 extracted with 4 different solvents - verification of the concentration of chlorophyll standards
787 by atomic-absorption spectroscopy. *Biochimica Et Biophysica Acta* **975,** 384-394.

788 Puerto-Galan L., Perez-Ruiz J.M., Ferrandez J., Cano B., Naranjo B., Najera V.A., ..., Cejudo
789 F.J. (2013) Overoxidation of chloroplast 2-cys peroxiredoxins: Balancing toxic and signaling
790 activities of hydrogen peroxide. *Frontiers in Plant Science* **4,** 310.

791 Pulido P., Cristina Spinola M., Kirchsteiger K., Guinea M., Belen Pascual M., Sahrawy M., ...,
792 Javier Cejudo F. (2010) Functional analysis of the pathways for 2-cys peroxiredoxin
793 reduction in arabidopsis thaliana chloroplasts. *Journal of Experimental Botany* **61,** 4043-
794 4054.

795 Rey P., Sanz-Barrio R., Innocenti G., Ksas B., Courteille A., Rumeau D., ..., Farran I. (2013)
796 Overexpression of plastidial thioredoxins f and m differentially alters photosynthetic activity
797 and response to oxidative stress in tobacco plants. *Frontiers in Plant Science* **4,** 390.

798 Richter A.S., Peter E., Rothbart M., Schlicke H., Toivola J., Rintamäki E., ..., Grimm B. (2013)
799 Posttranslational influence of NADPH-dependent thioredoxin reductase C on enzymes in
800 tetrapyrrole synthesis. *Plant Physiology* **162,** 63-73.

801 Sanz-Barrio R., Corral-Martinez P., Ancin M., Segui-Simarro J.M. & Farran I. (2013)
802 Overexpression of plastidial thioredoxin f leads to enhanced starch accumulation in tobacco
803 leaves. *Plant Biotechnology Journal* **11,** 618-627.

804 Sanz-Barrio R., Fernandez-San Millan A., Carballeda J., Corral-Martinez P., Segui-Simarro J.M.
805 & Farran I. (2012) Chaperone-like properties of tobacco plastid thioredoxins f and m.
806 *Journal of Experimental Botany* **63,** 365-379.

807 Schneider C.A., Rasband W.S. & Eliceiri K.W. (2012) NIH image to ImageJ: 25 years of image
808 analysis. *Nature Methods* **9,** 671-675.

809 Schürmann P. & Buchanan B.B. (2008) The ferredoxin/thioredoxin system of oxygenic
810 photosynthesis. *Antioxidants & Redox Signaling* **10,** 1235-1273.

811 Schwarz O., Schürmann P. & Strotmann H. (1997) Kinetics and thioredoxin specificity of thiol
812 modulation of the chloroplast H+-ATPase. *Journal of Biological Chemistry* **272,** 16924-
813 16927.

814 Serrato A.J., Fernandez-Trijueque J., Barajas-Lopez J.D., Chueca A. & Sahrawy M. (2013)
815 Plastid thioredoxins: A "one-for-all" redox-signaling system in plants. *Frontiers in Plant*
816 *Science* **4,** 463.

817 Serrato A.J., Perez-Ruiz J.M., Spinola M.C. & Cejudo F.J. (2004) A novel NADPH thioredoxin
818 reductase, localized in the chloroplast, which deficiency causes hypersensitivity to abiotic
819 stress in arabidopsis thaliana. *Journal of Biological Chemistry* **279,** 43821-43827.

820 Stitt M., Lunn J. & Usadel B. (2010) Arabidopsis and primary photosynthetic metabolism - more
821 than the icing on the cake. *Plant Journal* **61,** 1067-1091.

822 Thormählen I., Meitzel T., Groysman J., Ochsner A.B., von Roepenack-Lahaye E., Naranjo B.,
823 ..., Geigenberger P. (2015) Thioredoxin f1 and NADPH-dependent thioredoxin reductase C
824 have overlapping functions in regulating photosynthetic metabolism and plant growth in
825 response to varying light conditions. *Plant Physiology*.

826 Thormählen I., Ruber J., Von Roepenack-Lahaye E., Ehrlich S., Massot V., Huemmer C., ...,
827 Geigenberger P. (2013) Inactivation of thioredoxin f1 leads to decreased light activation of
828 ADP-glucose pyrophosphorylase and altered diurnal starch turnover in leaves of arabidopsis
829 plants. *Plant Cell and Environment* **36,** 16-29.

830 Toivola J., Nikkanen L., Dahlström K.M., Salminen T.A., Lepistö A., Vignols F., ..., Rintamäki
831 E. (2013) Overexpression of chloroplast NADPH-dependent thioredoxin reductase in
832 arabidopsis enhances leaf growth and elucidates in vivo function of reductase and
833 thioredoxin domains. *Frontiers in Plant Science* **4,** 389.

834 Voinnet O., Rivas S., Mestre P. & Baulcombe D. (2003) An enhanced transient expression
835 system in plants based on suppression of gene silencing by the p19 protein of tomato bushy
836 stunt virus. *Plant Journal* **33,** 949-956.

837 Waadt R. & Kudla J. (2008) In planta visualization of protein interactions using bimolecular
838 fluorescence complementation (BiFC). *CSH Protocols* **2008,** pdb.prot4995-pdb.prot4995.

839 Walter M., Chaban C., Schutze K., Batistic O., Weckermann K., Nake C., ..., Kudla J. (2004)
840 Visualization of protein interactions in living plant cells using bimolecular fluorescence
841 complementation. *Plant Journal* **40,** 428-438.

842 Wang P., Liu J., Liu B., Da Q., Feng D., Su J., ..., Wang H. (2014) Ferredoxin: Thioredoxin
843 reductase is required for proper chloroplast development and is involved in the regulation of
844 plastid gene expression in arabidopsis thaliana. *Molecular Plant* **7,** 1586-1590.

845 Wang P., Liu J., Liu B., Feng D., Da Q., Wang P., ..., Wang H. (2013) Evidence for a role of
846 chloroplastic m-type thioredoxins in the biogenesis of photosystem II in arabidopsis. *Plant*
847 *Physiology* **163,** 1710-1728.

848 Wolosiuk R., Crawford N., Yee B. & Buchanan B. (1979) Isolation of 3 thioredoxins from
849 spinach leaves. *Journal of Biological Chemistry* **254,** 1627-1632.

850 Yoshida K., Hara S. & Hisabori T. (2015) Thioredoxin selectivity for thiol-based redox
851 regulation of target proteins in chloroplasts. *The Journal of Biological Chemistry*.

852

853

Table 1. CO_2 fixation parameters of NTRC-overexpressing lines.

The parameters were calculated from the model $P_N = (I \times P_{gmax}) / (I + I_{50}) - R_D$ (Kaipiainen 2009). P_N = net photosynthetic rate, P_{gmax} = maximum gross photosynthetic rate, I_{comp}=light compensation point, I_{50} = light intensity where $P_N + R_D$ equals 50% of P_{Nmax}, R_D = dark respiration rate. The unit for P_{gmax} and R_D is µmol CO_2 $m^{-2}s^{-1}$ and for I_{comp} and I_{50} µmol photons $m^{-2}s^{-1}$.

Parameter	WT	OE-NTRC	OE-SAIS	OE-SGPS
P_{gmax}	7,1	8,5	10,9	9,4
I_{comp}	7,7	7,9	18,5	11,0
I_{50}	88,0	84,5	203,7	98,2
R_D	0,6	0,7	0,9	0,9

FIGURE LEGENDS

Figure 1. Phenotypes of plants overexpressing wild type and redox-inactive forms of NTRC.

(A) 6-weeks-old plants grown in 8h photoperiod under 500 µmol photons $m^{-2}s^{-1}$. (B) 8-weeks-old plants grown in 8h photoperiod under 100 µmol photons $m^{-2}s^{-1}$. (C) Immunoblot showing NTRC content in the transgenic lines. The quantifications were made by normalising the intensity of the NTRC band with the intensity of Coomassie-stained band of the Rubisco large subunit (RbcL) and with the amount of soluble protein loaded on the gel (µg, lower panel) as indicated in the figure. The relative amount of NTRC when compared to WT is shown in the middle panel of the image. The immunoblot shown and the quantifications are representative of three biological replicates.

Figure 2. Photosynthetic parameters of transgenic lines overexpressing wild-type and mutated NTRC

Chl fluorescence and P700 oxidation were measured from detached mature dark-adapted leaves of 5-week-old-plants grown under 500 µmol photons $m^{-2}s^{-1}$ in a short day photoperiod. Light response curves of quantum yield of PSI ([Y(I)] (A), acceptor side limitation of PSI [Y(NA)] (B), excitation pressure of PSII (1-qP) (C) and non-photochemical quenching (NPQ) (D), as well as induction curves with actinic light of 38 µmol photons $m^{-2}s^{-1}$ for Y(I) (E) and Y(NA) (F). PPFD=photosynthetic photon flux density. Values are means of four to six biological replicates ±SE. In (A) the X-axis has been broken at 140 µmol photons $m^{-2}s^{-1}$ with higher light intensities being shown in the right part of the graphs.

890

891 Figure 3. Photosynthetic carbon fixation in leaves overexpressing wild type and mutated NTRC

892 (A) Light response curves of net photosynthesis rates measured as μmol CO_2 $m^{-2}s^{-1}$ and fitted
893 into the model $P_N=(I \times P_{MAX})/(I+I_{50})-R_D$ (Kaipiainen 2009). (B) Light response curves of
894 photosynthetic quantum yield. Only light intensities 0–250 μmol photons $m^{-2}s^{-1}$ are shown. (C)
895 Light response curves of stomatal conductance. (D) Light response curves of intercellular CO_2
896 concentration. (B) to (D) are calculated from the measurements presented in (A). Values in (A)–
897 (D) are means from six to ten individual measurements from different leaves ±SE.

898

899 Figure 4. Interactions between NTRC and the Fd-TRX system.

900 (A) Merged Chl (red) and YFP (yellow) fluorescence images of BiFC tests showing *in planta*
901 interactions between NTRC and chloroplast TRXs or the catalytic subunit of FTR (FTRc). The
902 images shown are representative of three independent BiFC tests of similar results. (B) Gel shift
903 assay showing *in vivo* redox state of TRXf. Plants were illuminated in 0, 25, and 500 μmol
904 photons $m^{-2}s^{-1}$ before extraction of proteins, alkylation of reduced thiols with 4-Acetamido-4'-
905 Maleimidylstilbene-2,2'-Disulfonic Acid (AMS) and separation with non-reducing SDS-PAGE.
906 AMS indicates the control sample not treated with AMS. The proportion of reduced TRXf (%,
907 below the immunoblot) was quantified by calculating of the percentual proportion of reduced
908 TRXf (TRXf red.) from total TRXf (TXFf red. +TRXf ox.) in each sample.

909

910 Figure 5. Co-immunoprecipitation of chloroplast proteins with NTRC.

OE-NTRC and *ntrc* indicate crude lysates from OE-NTRC and *ntrc* knockout leaves, respectively, while w7 indicates the final washing step before elution and e the eluate from a co-immunoprecipitation column crosslinked with the NTRC antibody. Lysate, wash and eluate samples were separated with SDS-PAGE and the gel subsequently stained with Sypro Ruby protein stain (A) or blotted and the membrane probed with antibody against (B) NTRC, (C) large subunit of Rubisco (RbcL), (D) TRXf, (E) $CF_1\gamma$, (F) PRK or (G) FBPase. The two NTRC bands in (B) derive from monomeric and dimeric protein (Toivola et al. 2013). Similarly, as TRXf has a tendency to form oligomers (Sanz-Barrio et al. 2012), the highly acidic pH of the elution buffer likely causes most TRXf in the eluate to oligomerize, and only a minor proportion migrates on the gel as monomeric TRXf at ~12 kDa in (D). In (F) PRK migrates at ~40 kDa, with the lower band representing partly degraded protein. Two µg of protein was loaded on gels, except in (B), where 0.5 µg of OE-NTRC eluate was loaded. 50µl of wash solutions and *ntrc* eluate was loaded, because the protein content of these samples was below detection level (see materials and methods).

Figure 6. Effects of NTRC overexpression or mutation on the activation state of the chloroplast ATP synthase.

(A) ECS decay kinetics in leaves of NTRC-overexpressing and deficient transgenic plants. The red and black curves represent measurements from light- and dark-adapted leaves, respectively. The dark-adapted ECS values have been normalized in relation to the maximum value of the light-adapted leaves of each line. The dashed lines represent the time point where the ECS signal in dark-adapted leaves has diminished to 50 % of the maximum value. (B) Gel shift assay of

$CF_1\gamma$ redox state in the transgenic lines. Plant were illuminated in 0, 50, 500 and 1000 (1k) µmol photons $m^{-2}s^{-1}$ before extraction of proteins, -DTT indicates the negative control sample not treated with DTT prior to MAL-PEG incubation (see materials and methods), while Ox is oxidized and Red. the reduced form of $CF_1\gamma$. A representative immunoblot from three independent biological replicates is shown in the figure. See Supporting Information Table S2 for quantification of the data. (C) Merged Chl and YFP fluorescence images of BiFC tests for interactions between $CF_1\gamma$ and NTRC, TRXf1 or TRXx. For experimental details see the legend for Figure 4.

Figure 7. Redox states of plastidial thiol-regulated enzyme pools in the transgenic lines and interactions between TRXs and PRK or FBPase

(A) Gel shift assays of PRK, FBPase, and 2-Cys-PRX in the transgenic lines. Plants were illuminated in 0, 50, 500 or 1000 (1k) µmol photons $m^{-2}s^{-1}$ (PPFD) before extraction and MAL-PEG labelling of proteins. -DTT indicates the negative control sample not treated with DTT prior to MAL-PEG incubation (see materials and methods). The lowest MW band in the 2-Cys Prx blot represents a completely reduced form of 2-Cys Prxs (Red.), which cannot bind MAL-PEG. The middle band derives from 2-Cys Prx dimers (Red./Ox.) where one of the two intermolecular disulphides between peroxidatic (S_p) and resolving cysteines (S_r) has been reduced, i.e. the active form of the enzyme, while the upper band represents completely oxidized 2-Cys Prx (Ox.) with disulphide bridges connecting both cysteine pairs in the dimer (Puerto-Galan et al. 2013). The immunoblots shown are representative of four to six independent experiments. See Supporting Information Table S2 for quantification of the data. (B) Merged Chl and YFP images of BiFC

955 tests for interactions between PRK or FBPase and NTRC, TRXf1 or TRXx. For experimental
956 details see the legend for Figure 4.

957

958 Figure 8. A hypothetical model for the dynamics of TRX-mediated activation of ATP synthesis
959 and Calvin–Benson cycle in WT (A), OE-NTRC (B), OE-SAIS (C) and OE-SGPS (D) plants.

960 (A) In low light, when the electron flow in thylakoids is limited, the reduction of NTRC by
961 NADPH exceeds the reduction of FTR by Fd in WT leaves. Thus NTRC is mainly responsible
962 for initial activation of the ATP synthase and the CBC enzymes under limiting light conditions
963 and at the dark/light transition. In moderate light intensity the FTR-TRX system becomes more
964 active. NTRC is primary reductant of 2-Cys-PRXs in order to maintain redox homeostasis in the
965 chloroplast and to avoid oxidative stress that can induce inactivation of CBC enzymes. (B) In the
966 OE-NTRC line the reduction of CBC enzymes, ATP synthase, 2-Cys PRXs and free TRXs is
967 more effective than in wild type both in low and moderate light intensities. (C) and (D) The
968 mutated NTRC-overexpression lines suffer from oxidative stress and mutated NTRC competes
969 with other TRXs for binding with FTR (red lines), which decreases reducing capacity especially
970 in OE-SAIS plants. Due to the high accumulation of ROS the oxidized forms of redox regulated
971 CBC-enzymes dominate also in moderate light intensities. The solid and dashed arrows indicate
972 more and less effective reduction, respectively. The number of stars implies activation state of
973 the CBC or ATP synthesis. Ferredoxin (Fd) donates electrons to several acceptors but for
974 simplicity only the electrons directed to FTR and FNR are shown in the figure. LL refers to low
975 and ML to moderate light.

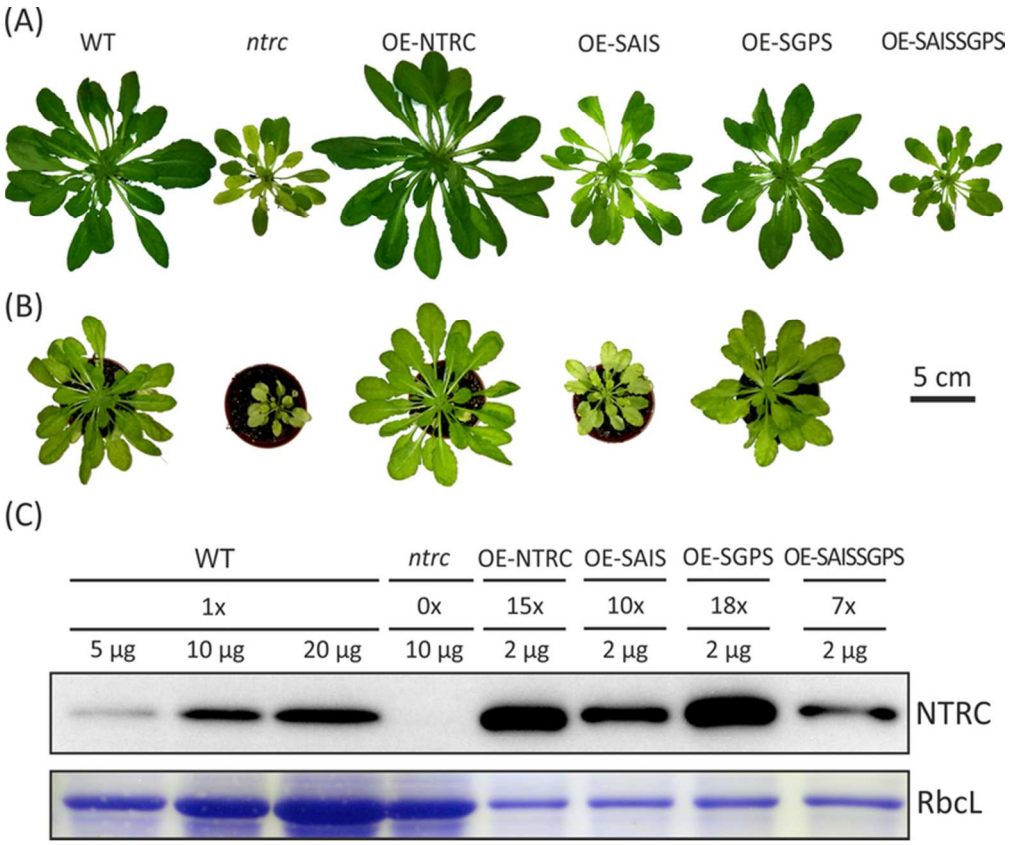

Figure 1. Phenotypes of plants overexpressing wild type and redox-inactive forms of NTRC. (A) 6-weeks-old plants grown in 8h photoperiod under 500 µmol photons $m^{-2}s^{-1}$. (B) 8-weeks-old plants grown in 8h photoperiod under 100 µmol $m^{-2}s^{-1}$. (C) Immunoblot showing NTRC content in the transgenic lines. The quantifications were made by normalising the intensity of the NTRC band with the intensity of Coomassie-stained band of the Rubisco large subunit (RbcL) and with the amount of soluble protein loaded on the gel (µg, lower panel) as indicated in the figure. The relative amount of NTRC when compared to WT is shown in the middle panel of the image. The immunoblot shown and the quantifications are representative of three biological replicates.
68x56mm (300 x 300 DPI)

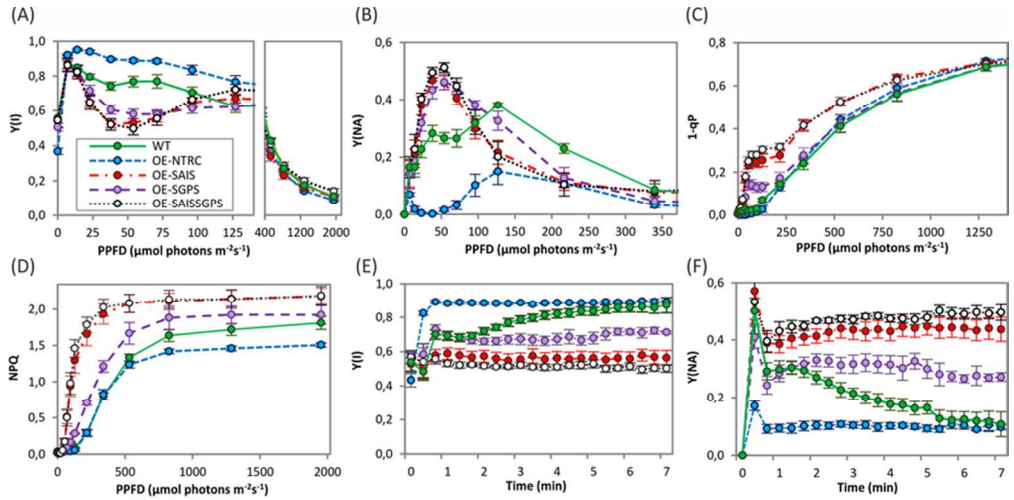

Figure 2. Photosynthetic parameters of transgenic lines overexpessing wild-type and mutated NTRC\nChl fluorescence and P700 oxidation were measured from detached mature dark-adapted leaves of 5-week-old-plants grown under 500 µmol photons $m^{-2}s^{-1}$ in a short day photoperiod. Light response curves of quantum yield of PSI ([Y(I)] (A), acceptor side limitation of PSI [Y(NA)] (B), excitation pressure of PSII (1-qP) (C) and non-photochemical quenching (NPQ) (D), as well as induction curves with actinic light of 38 µmol photons $m^{-2}s^{-1}$ for Y(I) (E) and Y(NA) (F). PPFD=photosynthetic photon flux density. Values are means of four to six biological replicates ±SE. In (A) the X-axis has been broken at 140 µmol $m^{-2}s^{-1}$ with higher light intensities being shown in the right part of the graphs.
77x38mm (300 x 300 DPI)

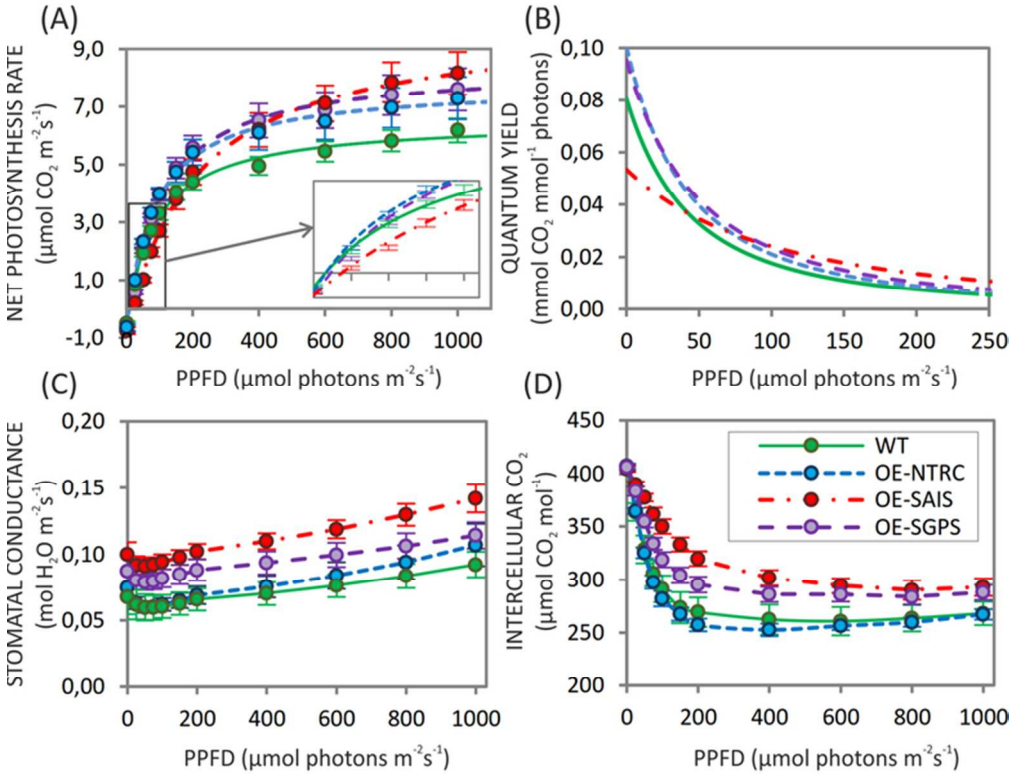

Figure 3. Photosynthetic carbon fixation in leaves overexpressing wild type and mutated NTRC (A) Light response curves of net photosynthesis rates measured as µmol CO_2 $m^{-2}s^{-1}$ and fitted into the model PN=(I x PMAX)/(I+I50)–RD (Kaipiainen 2009). (B) Light response curves of photosynthetic quantum yield. Only light intensities 0–250 µmol photons $m^{-2}s^{-1}$ are shown. (C) Light response curves of stomatal conductance. (D) Light response curves of intercellular CO_2 concentration. (B) to (D) are calculated from the measurements presented in (A). Values in (A)–(D) are means from six to ten individual measurements from different leaves ±SE.
65x50mm (300 x 300 DPI)

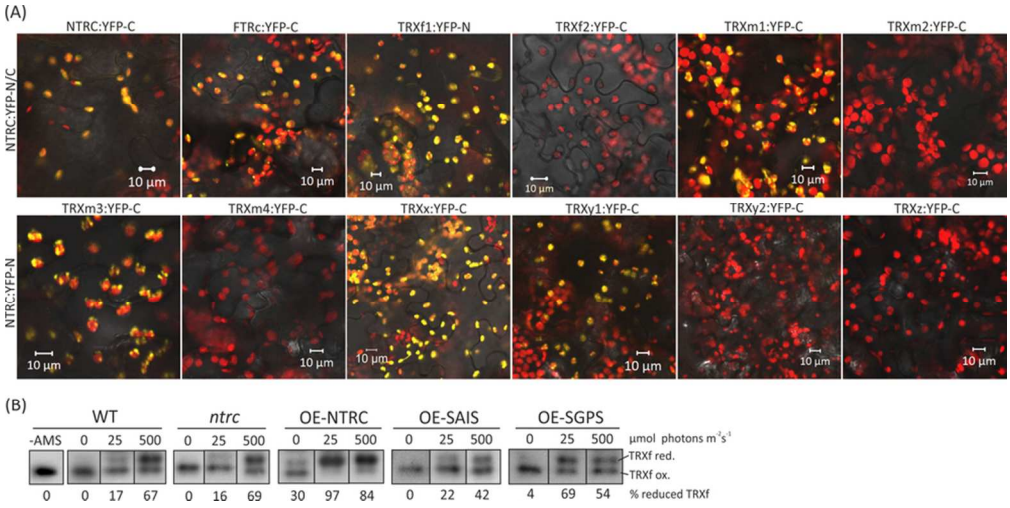

Figure 4. Interactions between NTRC and the Fd-TRX system.(A) Merged Chl (red) and YFP (yellow) fluorescence images of BiFC tests showing in planta interactions between NTRC and chloroplast TRXs or the catalytic subunit of FTR (FTRc). The images shown are representative of three independent BiFC tests of similar results. (B) Gel shift assay showing in vivo redox state of TRXf. Plants were illuminated in 0, 25, and 500µmol photons $m^{-2}s^{-1}$ before extraction of proteins, alkylation of reduced thiols with 4-Acetamido-4\'-Maleimidylstilbene-2,2\'-Disulfonic Acid (AMS) and separation with non-reducing SDS-PAGE. AMS indicates the control sample not treated with AMS. The proportion of reduced TRXf (% below the immunoblot) was quantified by calculating of the percentual proportion of reduced TRXf (TRXf red.) from total TRXf (TXFf red. +TRXf ox.) in each sample.
83x41mm (300 x 300 DPI)

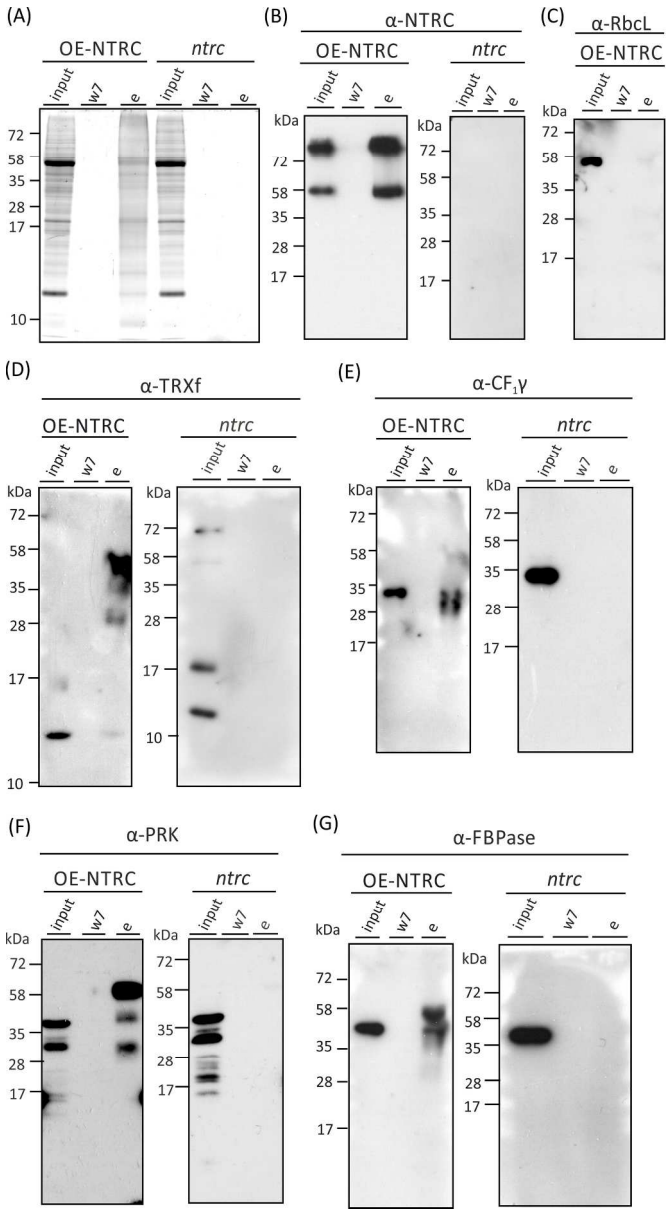

Figure 5. Co-immunoprecipitation of chloroplast proteins with NTRC. OE-NTRC and ntrc indicate crude lysates from OE-NTRC and ntrc knockout leaves, respectively, while w7 indicates the final washing step before elution and e the eluate from a co-immunoprecipitation column crosslinked with the NTRC antibody. Lysate, wash and eluate samples were separated with SDS-PAGE and the gel subsequently stained with Sypro Ruby protein stain (A) or blotted and the membrane probed with antibody against (B) NTRC, (C) large subunit of Rubisco (RbcL), (D) TRXf, (E) CF1γ, (F) PRK or (G) FBPase. The two NTRC bands in (B) derive from monomeric and dimeric protein (Toivola et al. 2013). Similarly, as TRXf has a tendency to form oligomers (Sanz-Barrio et al. 2012), the highly acidic pH of the elution buffer likely causes most TRXf in the eluate to oligomerize, and only a minor proportion migrates on the gel as monomeric TRXf at ~12 kDa in (D). In (F) PRK migrates at ~40 kDa, with the lower band representing partly degraded protein. Two µg of protein was loaded on gels, except in (B), where 0.5 µg of OE-NTRC eluate was loaded. 50µl of wash solutions and ntrc eluate was loaded, because the protein content of these samples was below detection level (see materials and methods).

154x281mm (300 x 300 DPI)

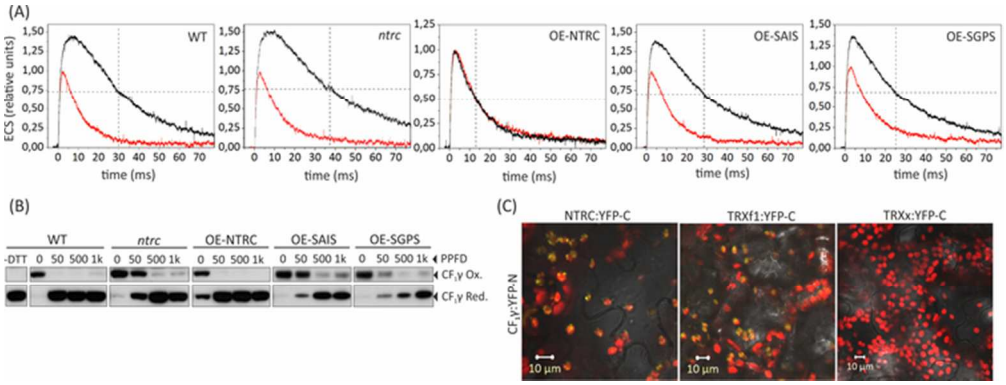

Figure 6. Effects of NTRC overexpression or mutation on the activation state of the chloroplast ATP synthase. (A) ECS decay kinetics in leaves of NTRC-overexpressing and deficient transgenic plants. The red and black curves represent measurements from light- and dark-adapted leaves, respectively. The dark-adapted ECS values have been normalized in relation to the maximum value of the light-adapted leaves of each line. The dashed lines represent the time point where the ECS signal in dark-adapted leaves has diminished to 50 % of the maximum value. (B) Gel shift assay of CF1γ redox state in the transgenic lines. Plant were illuminated in 0, 50, 500 and 1000 (1k) µmol photons $m^{-2}s^{-1}$ before extraction of proteins, -DTT indicates the negative control sample not treated with DTT prior to MAL-PEG incubation (see materials and methods), while Ox is oxidized and Red. the reduced form of CF1γ. A representative immunoblot from three independent biological replicates is shown in the figure. See Supporting Information Table S2 for quantification of the data. (C) Merged Chl and YFP fluorescence images of BiFC tests for interactions between CF1γ and NTRC, TRXf1 or TRXx. For experimental details see the legend for Figure 4.
63x23mm (300 x 300 DPI)

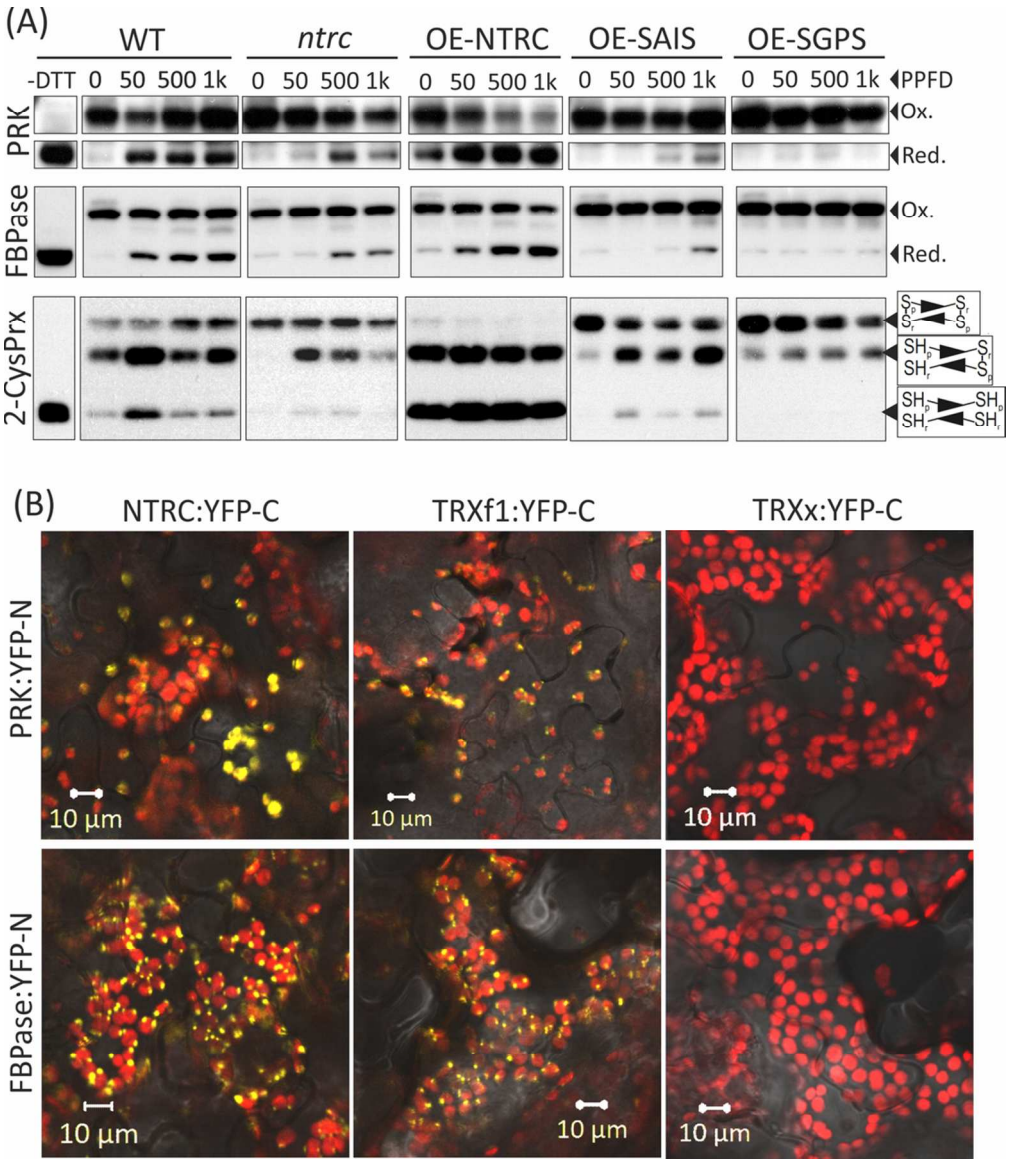

Figure 7. Redox states of plastidial thiol-regulated enzyme pools in the transgenic lines and interactions between TRXs and PRK or FBPase (A) Gel shift assays of PRK, FBPase, and 2-Cys-PRX in the transgenic lines. Plants were illuminated in 0, 50, 500 or 1000 (1k) µmol photons $m^{-2}s^{-1}$ (PPFD) before extraction and MAL-PEG labelling of proteins. -DTT indicates the negative control sample not treated with DTT prior to MAL-PEG incubation (see materials and methods). The lowest MW band in the 2-Cys Prx blot represents a completely reduced form of 2-Cys Prxs (Red.), which cannot bind MAL-PEG. The middle band derives from 2-Cys Prx dimers (Red./Ox.) where one of the two intermolecular disulphides between peroxidatic (Sp) and resolving cysteines (Sr) has been reduced, i.e. the active form of the enzyme, while the upper band represents completely oxidized 2-Cys Prx (Ox.) with disulphide bridges connecting both cysteine pairs in the dimer (Puerto-Galan et al. 2013). The immunoblots shown are representative of four to six independent experiments. See Supporting Information Table S2 for quantification data. (B) Merged Chl and YFP images of BiFC tests for interactions between PRK or FBPase and NTRC, TRXf1 or TRXx. For experimental details see the legend for Figure 4.
98x113mm (300 x 300 DPI)

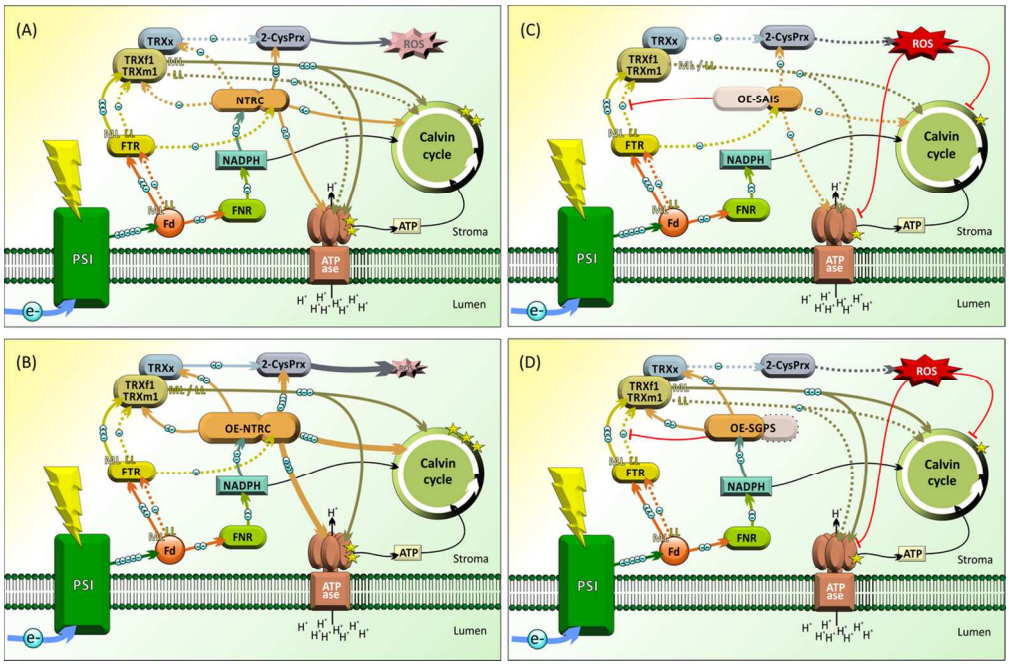

Figure 8. A hypothetical model for the dynamics of TRX-mediated activation of ATP synthesis and Calvin–Benson cycle in WT (A), OE-NTRC (B), OE-SAIS (C) and OE-SGPS (D) plants. \n(A) In low light, when the electron flow in thylakoids is limited, the reduction of NTRC by NADPH exceeds the reduction of FTR by Fd in WT leaves. Thus NTRC is mainly responsible for initial activation of the ATP synthase and the CBC enzymes under limiting light conditions and at the dark/light transition. In moderate light intensity the FTR-TRX system becomes more active. NTRC is primary reductant of 2-Cys-PRXs in order to maintain redox homeostasis in the chloroplast and to avoid oxidative stress that can induce inactivation of CBC enzymes. (B) In the OE-NTRC line the reduction of CBC enzymes, ATP synthase, 2-Cys PRXs and free TRXs is more effective than in wild type both in low and moderate light intensities. (C) and (D) The mutated NTRC-overexpression lines suffer from oxidative stress and mutated NTRC competes with other TRXs for binding with FTR (red lines), which decreases reducing capacity especially in OE-SAIS plants. Due to the high accumulation of ROS the oxidized forms of redox regulated CBC-enzymes dominate also in moderate light intensities. The solid and dashed arrows indicate more and less effective reduction, respectively. The number of stars implies activation state of the CBC or ATP synthesis. Ferredoxin (Fd) donates electrons to several acceptors but for simplicity only the electrons directed to FTR and FNR are shown in the figure. LL refers to low and ML to moderate light.
114x75mm (300 x 300 DPI)